



A Comparative Soil Liquefaction Analysis with a MATLAB® based Algorithm: soiLique

Ekrem Bekin^{1,2}, Ferhat Ozcep²

¹Memorial University of Newfoundland, Canada.

²Istanbul University – Cerrahpasa, Turkey.

Corresponding author: ebekin@mun.ca

ABSTRACT

Soil liquefaction is one of the ground failures induced by earthquakes. Determining the safety factor and the settlements are the most common analyses to decrease liquefaction-induced failures and hazards. Scientists have suggested numerous empirical formulas to detect and mitigate liquefaction-based hazards, and they have been used over the decades. This study aims to present a user-friendly and interactive program for deterministic soil liquefaction analyses. The algorithm presented in this study, soiLique, is the first MATLAB® program, including a graphical user interface that provides the deterministic liquefaction analysis with the computation of parameters propounded with the formulas. One of the advantages of soiLique is that it allows picking the physical property of every layer (i.e., fine or coarse), which provides dealing with liquefaction prone layer(s) directly when necessary. Not only can one calculate parameters regarding soil liquefaction with the help of this program, but one also can see graphically supported results. The robustness of soiLique is checked with another soil liquefaction analysis program, SoilEngineering, which was introduced by Ozcep (2010). Calculations were done separately using real SPT data and synthetic data such as V_s measurements and CPT data. The real SPT data and synthetic VS data were used to compare soiLique and SoilEngineering (Ozcep, 2010). The present study presents an example of CPT data analysis but could not be used for comparison. Comparisons reveal that outputs of soiLique and results of SoilEngineering showed a good agreement.

Keywords: Soil Liquefaction; Soil Engineering; Soil Dynamics; Soil Properties; Field Tests; Natural Hazards; Earthquakes; Graphical User Interface; MATLAB®-GUI.

Análisis comparativo de licuación del suelo con un algoritmo basado en Matlab®: soiLique

RESUMEN

La licuación del suelo es un corrimiento del terreno inducido por movimientos sísmicos. La determinación del factor de seguridad y de los asentamientos son los análisis más comunes para reducir las fallas y las amenazas causadas por la licuación. Numerosas formulas empíricas han sido sugeridas por expertos para detectar y mitigar los riesgos de licuación, y estas han sido usadas por décadas. Este estudio busca presentar un programa interactivo y de fácil uso para los análisis determinísticos de licuación del suelo. El algoritmo presentado en este estudio, soiLique, es el primer programa basado en Matlab® e incluye una interfaz gráfica de usuario que provee el análisis determinístico de licuación con los parámetros de computación propuestos con las formulas. Una de las ventajas de soiLique es que brinda la oportunidad de elegir las propiedades físicas de cada capa (por ejemplo, fina o gruesa), lo que permitiría tratar directamente con las capas propensas a la licuación cuando sea necesario. No solo se pueden calcular los parámetros relacionados a la licuación del suelo con la ayuda de este programa sino que además se pueden ver gráficamente los resultados. La robustez de soiLique se verificó con otro programa de análisis de licuación del suelo, SoilEngineering, que fue introducido por Ozcep en 2010. Se hicieron cálculos separados con información real de Pruebas Estándares de Penetración (SPT, del inglés Standar Penetration Test), información sintética de Velocidad de Onda de Corte Medida (V_s , del inglés Measured Shear Wave Velocity) e información de Pruebas de Penetración Cónica (CPT, del inglés Conic Penetration Test). La información real SPT y la información sintética VS fueron usadas para comparar los resultados de soiLique y SoilEngineering. En este estudio se presentan un ejemplo de información CPT pero no se usa en la comparación. Las comparaciones muestran que la información arrojada por soiLique y los resultados de SoilEngineering muestran concordancia.

Palabras clave: Licuación del suelo; Ingeniería de suelos; dinámicas de suelos; propiedades del suelo; pruebas de campo; Riesgos Naturales; terremotos; interfaz gráfica de usuario; Matlab®

Record

Manuscript received: 22/04/2020

Accepted for publication: 12/03/2021

How to cite item

Bekin, E., & Ozcep, F. (2021). A Comparative Soil Liquefaction Analysis with a MATLAB® based Algorithm: soiLique. *Earth Sciences Research Journal*, 25(3), 323-340. DOI: <https://doi.org/10.15446/esrj.v25n3.86525>

Nomenclature

α : Standard Penetration Test Blow Count Correction Coefficient with respect to Fine Content

β : Standard Penetration Test Blow Count Correction Coefficient with respect to Fine Content

Δ : Focal Depth

ϵ_v : Volumetric Strain

γ : Unit Volume Weight

σ, σ_0 : Total vertical stress

σ', σ'_0 : Vertical effective stress

a_{max} : Peak Ground Acceleration

C_n : Depth Correction Factor

C_b : Borehole Correction Factor

C_e : Hammer Energy Ratio

C_r : Rod Length Correction Factor

C_s : Correction Factor for Samples with/without liners

C_v : Factor to correct measured shear wave velocity

CPT: Conic Penetration Test

CRR: Cyclic Resistance Ratio

$CRR_{7.5}$: Cyclic Resistance Ratio

CSR: Cyclic Stress Ratio

D_R : Relative Density

FC: Fine Content

f_s : Sleeve Friction

GUI: Graphical User Interface

h : Projection of the Earthquake Source to Earth's Surface

h_w : Water Table Level

I_c : Soil Behaviour Type Index

M : Earthquake Magnitude

M_j : Earthquake Magnitude defined by Japan Meteorological Association

M_L : Local Magnitude

M_w : Moment Magnitude

MSF: Magnitude Scaling Factor

N_{mea} : Measured Standard Penetration Test Blow Count

$(N_1)_{60}$: Corrected Standard Penetration Test Blow Count

$(N_1)_{60FC}$: Standard Penetration Test Blow Count Corrected with respect to Fine Content

q_c : Tip Resistance

q_{c1} : Corrected Tip Resistance

q_{c1F} : Tip Resistance Corrected with respect to Fine Content

P_a : Reference Stress of 100 kPa or about Atmospheric Pressure

r_d : Stress Reduction Coefficient

R_f : Sleeve Friction Ratio

SF: Safety Factor

SPT: Standard Penetration Test

V_s : Measured Shear Wave Velocity

V_{s1} : Corrected Shear Wave Velocity

z : Depth

1. Introduction

The assessment of the soil resistance against liquefaction or the amount of settlement of an engineered building caused by liquefaction is a remarkable phase concerning geotechnical and geophysical investigations. In earthquake-prone areas, during dynamic loading, i.e., an earthquake, pore water pressure increases in undrained and cohesionless soils. Therefore, these materials lose their solid behavior and act as if liquefied materials (Terzaghi and Peck, 1948; Ishihara and Yoshimine, 1992; Bekin and Ozcep, 2017). In general, the earthquake hazard risk increases because of liquefied behavior. Because of having great importance on engineered buildings and hence having a significant impact on natural hazards, researchers have studied the liquefaction phenomenon after the 1964 Niigata Earthquake.

From the fundamental theoretical background point of view, scientists have been proposed empirical relationships to determine the probable effects and to reduce the hazard levels based on liquefaction for more than 30 years. For example, Liao and Whitman (1986) have introduced the stress reduction coefficient (r_d) to calculate the cyclic stress ratio (CSR). Youd and Idriss (1997)

have presented a better way to compute CSR in their study. Andrus and Stokoe (2000) have formulated the relationship between the shear wave velocity (V_s) and the cyclic resistance ratio (CRR). Youd et al. (2001) have demonstrated the relationship between CRR and corrected Standard Penetration Test (SPT) blow count numbers $(N_1)_{60}$. Tokimatsu and Seed (1987) have presented formulas to calculate the amount of expected settlement for liquefaction vulnerable regions dependent on $(N_1)_{60}$. Likely, Ishihara and Yoshimine (1992) have proposed empirical formulas for settlements with respect to $(N_1)_{60}$ values and corrected tip resistance (q_{c1}) values of CPT.

The target of this study is to present a deterministic liquefaction analysis routine, *soiLique*, with a graphical user interface (GUI). This routine is the first MATLAB® based soil liquefaction analysis routine. The program presented in this study, *soiLique*, includes several approaches for the assessment of the maximum extent of liquefaction-susceptible areas. Firstly, Kuribayashi and Tatsuoka (1975), Wakamatsu (1991), and Wakamatsu (1993) that have related M_j and the maximum distance for the liquefiable area (R). Although Liu and Xie (1984) have used M_L , Ambraseys (1988) have made use of M_w for the estimation. Additionally, Ulusay et al. (2000) have proposed the relation between M_s and the maximum distance R .

The results of *soiLique* were compared to the liquefaction analysis panel of another program, *SoilEngineering*, introduced by Ozcep (2010), to test the robustness of the algorithm. It is a widely used -especially in Turkey-, free access, and user-friendly Microsoft Excel® based program for the geotechnical and geophysical analysis of soils. It provides the user to prepare data, to derive parameters, and to carry out analysis of geotechnical and geophysical problems. The fundamental characteristic of *soiLique* is its independence from MATLAB®. In other words, *soiLique* can be used without MATLAB® by installing MATLAB® Runtime Environment v9.7 to run.

In the present study, the theory associated with *soiLique* is explained in the second chapter. The third chapter focuses mainly on the framework of *soiLique*. In the fourth chapter, the geological setting of the study area, where the real data are collected, and the analyses for checking the robustness of *soiLique* are presented. In addition to the tables and plots presented in the results and discussion section, readers can find some plots and more detailed tables in the supplementary file.

2. Theoretical Background

The theory associated with *soiLique* is explained in this section. There are various approaches and assessment methods to conduct a solution-oriented liquefaction analysis. Analyses that are mentioned in the present study can be classified as the assessment methods for the maximum extent of a liquefiable area, the calculations of settlements or prospective settlements, and liquefaction safety factor. These theoretical principles are represented in three sub-sections. In the first one, approaches of the maximum distance of a liquefiable area are explained. After that, safety factor analysis, including $CRR_{7.5}$ (Cyclic Resistance Ratio, subjected to $M_w=7.5$) and CSR (Cyclic Stress Ratio), calculations are presented as the second sub-section. In the next sub-section, calculations of the settlements triggered by liquefaction are explained. Lastly, a simple analysis method, which has been introduced by Tezcan and Teri (1996), is explained.

2.1. The Evaluation of a Maximum Extent of a Liquefiable Area

Several investigators have studied the spread of liquefaction during former earthquakes and proposed the relationship between the magnitude of an earthquake, M , and the maximum distance from the epicenter to the liquefied area, R . Liquefaction prone areas can be estimated immediately from the magnitude of the predicted earthquake with the help of these approaches if the seismic activity in the corresponding area is known from the historic earthquake catalog.

Kuribayashi and Tatsuoka (1975) have shown the relationship between magnitude and maximum epicentral distance to a liquefied site by using 32 historic Japanese earthquakes. The logarithmic relation can be expressed as:

$$\log R = 0.77 * M_j - 3.6 \quad (1)$$

where M_J is the earthquake magnitude scale defined by Japan Meteorological Association, R denotes the distance, in km, between the earthquake epicenter and the farthest liquefied site in km. Liu and Xie (1984) have proposed another relationship based on the Chinese liquefaction database concerning the local magnitude (M_L):

$$R = 0.82 * 10^{0.862(M_L - 5)} \quad (2)$$

where M_L is the earthquake magnitude defined by Richter (1935), and R is the maximum distance, in km, of the liquefied site to the epicenter.

Ambraseys (1988) has represented two different approaches to estimate the seismic moment magnitude (M_w) from a distance between the epicenter and liquefied site. In the first approach, Ambraseys (1988) has standardized the Equation 3 for shallow and intermediate-depth earthquakes. According to the study, earthquakes having intermediate-depths and the much longer duration of shaking may induce liquefaction at distances greater than those dictated by shallow-focused earthquakes. The data points R_c and M_w are bounded by the equation:

$$M_w = 4.64 + 2.65 * 10^{-3} * R_c + 0.99 * \log R_c \quad (3)$$

where R_c is the maximum epicentral distance, and M_w is the seismic moment magnitude. In the second approach, R_f is the closest distance from a shallow seismic source of the furthest point of liquefaction, as a function of seismic moment magnitude M_w .

Ambraseys (1988) has explained that the maximum fault distance R_p at which liquefaction may occur saturates at about $M_w = 8.0$, beyond which value R_p remains constant and equal to about 160 km. As one of the results of the study, Ambraseys has explained that it is rational for large shallow earthquakes where the maximum fault-depth remains constant without consideration of the fault-length, while M_w depends upon fault-length. The expression that defines the upper bound for R_p as a function of M_w can be given as:

$$M_w = 4.68 + 9.2 * 10^{-3} * R_f + 0.9 * \log R_f \quad (4)$$

where R_f is the maximum distance, in km, from causative fault to a liquefied site, and M_w is the seismic moment magnitude.

In addition to Kuribayashi and Tatsuoka (1975), Wakamatsu (1991) have shown the relationship between magnitude, and maximum epicentral distance to a liquefied site by using 67 historic Japanese earthquakes, including 32 earthquakes which were used by Kuribayashi and Tatsuoka (1975), the equation, which has bounded with $M_J > 5.0$, can be expressed as:

$$\log R = 2.22 * \log(4.22 * M_J - 19) \quad (5)$$

The Equation 5 has been revised, and Wakamatsu (1993) has presented a newer version of the equation to estimate the maximum range of liquefaction for specific earthquake magnitude. This relation can be given as:

$$\log R = 3.5 * \log(1.4 * M_J - 6) \quad (6)$$

where R is the farthest epicentral distance, in km, and M_J is the earthquake magnitude scale defined by Japan Meteorological Association.

Lastly, Ulusay et al. (2000) proposed the relationship between surface wave magnitude (M_s) and the maximum distance R of a liquefied site for the Turkey region. Ulusay et al. (2000) have come up with an empirical formula taking the upper and the lower boundaries in consideration addition to the calculation of average value to figure out M_s and R . In order to calculate a distance value (R_{CAL} , in km), one should use focal depth and another parameter that corresponds to a distance between the projection of the epicenter to the Earth's surface and the site subjected to liquefaction. The equation can be given as follows:

$$R_{CAL} = \sqrt{(\Delta^2 + h^2)} \quad (7)$$

where Δ represents the focal depth, and h stands for the projection of the earthquake source point to the Earth's surface. After that, surface wave magnitudes can be calculated by the following equations:

$$M_s = (R_{CAL} + 160) / 36 \quad (8)$$

$$M_s = (R_{CAL} + 200) / 36 \quad (9)$$

$$M_s = (R_{CAL} + 240) / 36 \quad (10)$$

where the expression given in Equation 8 is the lower boundary for the calculation, Equation 9 and Equation 10 are the medium value and the upper boundary of the magnitude calculation, respectively. From the point of R calculation view, the same procedure is valid. In other words, Equations 11, 12, and 13 are given for R calculation (in km) with the discrimination of the upper, medium value, and the lowest boundaries, respectively.

$$R = M_s * 36 - 160 \quad (11)$$

$$R = M_s * 36 - 200 \quad (12)$$

$$R = M_s * 36 - 240 \quad (13)$$

All of these theoretical approaches were used in the maximum extent of the liquefiable area analysis part in soiLique. Merely, the medium value boundary calculation is used in the approach mentioned in Ulusay et al. (2000).

2.2. Safety Factor Analysis

The safety factor is used to understand whether the investigation area is in the safe zone against liquefaction. Various approaches have been represented by investigators to estimate the safety factor of liquefaction. The fundamental step in finding the safety factor is the division of Cyclic Resistance Ratio (CRR) and Cyclic Stress Ratio (CSR). Hence, CSR and CRR must be calculated to mention the safety factor.

CSR, which is induced by a particular earthquake, was first introduced by Seed and Idriss (1967). It is an equivalent form of the uniform shear stress, which is triggered by the corresponding earthquake (Boulanger and Idriss, 2014). Seed and Idriss (1971) has introduced

CSR with a reference value equal to 65% of the peak cyclic stress. The empirical formula of CSR is given in Equation 14:

$$CSR = 0.65 * \frac{\sigma_0}{\sigma_0'} * a_{max} * r_d \quad (14)$$

where σ_0 is the total vertical overburden stress, σ_0' is the effective vertical overburden stress, a_{max} is the peak ground acceleration and r_d is a stress reduction coefficient which can be calculated by:

$$r_d = 1.0 - 0.00765 * z \quad z \leq 9.15 \text{ m} \quad (15)$$

$$r_d = 1.174 - 0.0267 * z \quad 9.15 \text{ m} < z \leq 23 \text{ m} \quad (16)$$

where z is the depth of the layer in m. The calculation of stress reduction coefficient, r_d , possesses other conditions for the depths of 30 m and greater. However, for cases where z is greater than 23 m, potential liquefiable layers may be neglected from the point of overburden stress view. Liquefaction assessments at greater depths frequently include specific conditions that need to be verified by detailed analyses. Because of that reason, Idriss and Boulanger (2008) have suggested completing site response studies by a high-quality site

response calculations for the sites where the r_d values at depths greater than approximately 20 m. That is the reason why it is used only for up to 23 m depth values in the present study.

CRR, cyclic resistance ratio, can be called the strength of the soil. Unlike CSR, CRR can be calculated from the Standard Penetration Test (SPT), Conic Penetration Test (CPT), and shear wave velocity (V_s) measurements. In general, CRR curves were firstly introduced for an earthquake having a moment magnitude equals 7.5, and its symbol is $CRR_{7.5}$. For different moment magnitude values, one must switch from $CRR_{7.5}$ to CRR, by multiplying it with a magnitude scaling factor (MSF). It can be given as:

$$MSF = 10^{2.24} / M_w^{2.56} \quad (17)$$

where M_w denotes the moment magnitude of an earthquake. Then, the safety factor, SF, can be calculated with the division of the CRR and CSR:

$$SF = CRR / CSR \quad (18)$$

2.2.1. Obtaining $CRR_{7.5}$ from SPT Data

In soilLique, the methodology mentioned in Seed and Idriss (1971) is used to obtain $CRR_{7.5}$. In the theory of SPT- $CRR_{7.5}$ computations, SPT data must be corrected before calculations. The formulation of SPT blow count correction can be given as:

$$(N_1)_{60} = N_{mea} * C_n * C_e * C_b * C_r * C_s \quad (19)$$

where the left-hand side of the equation represents the corrected SPT blow count, N_{mea} is the measured SPT blow counts in a field, C_n is the depth correction factor, C_e corresponds to hammer energy ratio (ER) correction factor, C_b is the borehole diameter correction factor, C_r denotes rod length correction factor, and C_s stands for correction factor for samplers with or without liners. Details of these corrections for SPT blow count given by Youd and Idriss (2001) are also represented in Table 1.

Table 1. Corrections for SPT blow count (modified from Youd and Idriss, 2001)

| Factor | Equipment Variable | Term | Correction |
|---------------------|----------------------------------|-------|--|
| Overburden Pressure | - | C_n | $C_n = 2.2 / (1.2 + \sigma'_{v0} / P_a)$ $C_n \leq 1.7$ |
| Energy Ratio | Safety Hammer | C_e | 0.5 - 1 |
| | Donut Hammer | | 0.7 - 1.2 |
| | Automatic Trip Donut Type Hammer | | 0.8 - 1.3 |
| Borehole Diameter | 65 - 115 mm | C_b | 1 |
| | 150 mm | | 1.05 |
| | 200 mm | | 1.15 |
| Total Rod Length | < 3 m | C_r | 0.75 |
| | 3 m to 4 m | | 0.8 |
| | 4 m to 6 m | | 0.85 |
| | 6 m to 10 m | | 0.95 |
| | 10 m to 30 m | | 1 |
| Sampling Method | Standard Sampler | C_s | 1 |
| | Sampler without Liners | | 1.1-1.3 |

Having the SPT N is corrected, the procedures stated in firstly Seed and Idriss (1971), and the fine content correction, which has been updated by Youd and Idriss (2001), is applied to calculate $CRR_{7.5}$. The procedure starts with the formula given below:

$$(N_1)_{60FC} = \alpha + \beta * (N_1)_{60} \quad (20)$$

and where α and β are:

$$\alpha = 0, \beta = 1 \quad F.C. \leq \%5 \quad (21)$$

$$\alpha = \exp[1.76 - (190 / FC^2)], \beta = 0.99 + FC^{1.5} / 1000 \quad \%5 < F.C. < \%35 \quad (22)$$

$$\alpha = 5, \beta = 1.2 \quad F.C. \geq \%35 \quad (23)$$

where F.C. means fine content. The Equations 21, 22, and 23 are used for calculation of the coefficients of fine content correction of SPT blow count, given in Equation 20, in terms of fines content percentage in the samples. Then, $CRR_{7.5}$ can be obtained with the formula:

$$CRR_{7.5} = \frac{1}{34 - (N_1)_{60FC}} + \frac{(N_1)_{60FC}}{135} + \frac{50}{(10 * (N_1)_{60FC} + 45)^2} - \frac{1}{200} \quad (24)$$

which has the upper limit at 30 for $(N_1)_{60FC}$ in (Youd and Idriss, 2001).

2.2.2. Obtaining $CRR_{7.5}$ from V_s Measurements

Shear-wave velocities (V_s) can be measured in situ with the help of several seismic techniques including cross hole, downhole, seismic cone penetrometer, suspension logger, SASW, and MASW. Their accuracy can be sensitive to processing details, soil conditions, and interpretation methods Andrus and Stokoe (2000). One can correct V_s to a reference overburden stress by (Sykora, 1987; Robertson et al. 1992)

$$V_{s1} = C_v * V_{sm} \quad (25)$$

where C_v = factor to correct measured shear-wave velocity for overburden pressure and can be calculated by

$$C_v = (P_a / \sigma'_0)^{0.25} \quad (26)$$

where V_{s1} is overburden stress-corrected shear-wave velocity, P_a is the reference stress of 100 kPa or about atmospheric pressure; and σ'_0 is the initial effective overburden stress (kPa). Then, $CRR_{7.5}$, based on V_s measurements, can be calculated by:

$$CRR_{7.5} = 0.022 * \left(\frac{V_{s1}}{100} \right)^2 + 2.8 * \left[\left(\frac{1}{215 - V_{s1}} \right) - \left(\frac{1}{215} \right) \right] \quad F.C. \leq \%5 \quad (27)$$

$$CRR_{7.5} = 0.022 * \left(\frac{V_{s1}}{100} \right)^2 + 2.8 * \left[\left(\frac{1}{215 - 0.5(FC - 5) - V_{s1}} \right) - \left(\frac{1}{215 - 0.5(FC - 5)} \right) \right] \quad (28)$$

$\%5 < F.C. < \%35$

$$CRR_{7.5} = 0.022 * \left(\frac{V_{s1}}{100} \right)^2 + 2.8 * \left[\left(\frac{1}{200 - V_{s1}} \right) - \left(\frac{1}{200} \right) \right] \quad F.C. \geq \%35 \quad (29)$$

where F.C. is the representative of the fine content (Andrus and Stokoe, 2000).

2.2.3. Obtaining $CRR_{7.5}$ from CPT Data

The $CRR_{7.5}$ calculation of CPT data in soilLique is based on the technique which was published by Suzuki et al. in 1997. This technique includes the computation of a soil behavior type index, I_c , and the adjustment of measured tip resistance with factor f_c . This factor is also a function of the soil behavior

type index. In this technique, the measured tip resistance is corrected in terms of overburden pressure with the formula given below:

$$q_{c1} = \frac{q_c \left(\frac{P_a}{\sigma_0} \right)^2}{P_a} \quad (30)$$

where q_{c1} is the corrected tip resistance, q_c is the measured one, σ_0' is the effective overburden stress (kPa), and P_a is the reference stress of 100 kPa or about atmospheric pressure. The next step is the calculation of the soil behavior index, which has been represented by Robertson et al. (1995) :

$$I_c = \left[(3.47 - \log Q)^2 + (\log R_f + 1.22)^2 \right]^{0.5} \quad (31)$$

where Q and R_f are:

$$Q = \frac{q_{c1f} - \sigma_0}{\sigma_0} \quad (32)$$

$$R_f = \frac{f_s}{q_{c1f} - \sigma_0} * 100 \quad (\%) \quad (33)$$

and where q_{c1f} is the fines corrected tip resistance in tsf, f_s is the measured sleeve friction, σ_0 is the total vertical overburden stress, σ_0' is the effective vertical overburden stress, Q is a normalized tip resistance, and R_f is a sleeve friction ratio. The last step before calculating the $CRR_{7.5}$ is the adjustment of the tip resistance, and it can be achieved by the formula as follows:

$$q_{ca} = q_{c1f} * f(I_c) \quad (34)$$

q_{ca} is equivalent to the adjusted tip resistance, and as it has already mentioned before, f is the function of soil behavior index and with the range between 1 and 3.5 depending on changing values of the soil behavior type index, I_c . For the values less than and equal to 1.65, $f(I_c)$ turns into one (1); and for values higher than and equal to 2.4, it takes 3.5. In the range between 1.65 and 2.4, it takes different values. In the present study, $CRR_{7.5}$ is calculated with the formula, which was proposed for the method of Suzuki et al. (1997), mentioned in Mollamahmutoglu and Babuccu (2006) instead of using $CRR_{7.5}$ liquefaction curve versus adjusted tip resistance given by Suzuki et al. (1997).

2.3. Settlement Analysis

If the safety factor of liquefaction is known, it is possible to determine the variation of the post-liquefaction volumetric strain (Ishihara and Yoshimine, 1992). The combination of safety factor and the volumetric strain was proposed by Ishihara and Yoshimine (1992), and it is given in Figure 1.

The relationship between corrected SPT blow count, $(N_1)_{60}$, and the post-liquefaction volumetric strain was proposed by Tokimatsu and Seed (1987). The combination can be read from Figure 2.

In the present study, equations introduced by Mollamahmutoglu and Babuccu (2006) are used to compute the possible post-liquefaction settlements. They have used the curve overlaying technique and proposed equations for both methods of (Ishihara and Yoshimine, 1992) and (Tokimatsu and Seed, 1987). The objective is the computation of possible post-liquefaction settlement after the estimation of volumetric strain. Settlements can be calculated with the formula below:

$$S_{sat} = (\varepsilon_v / 100) * z \quad (35)$$

where z is the thickness of the layer in m, ε_v is the volumetric strain, and S_{sat} signifies the corresponding saturated soil layer.

2.4. Simple Analysis

The relation between relative density (D_R), in percentages, and peak ground acceleration (PGA), in g, has been proposed by Tezcan and Teri (1996).

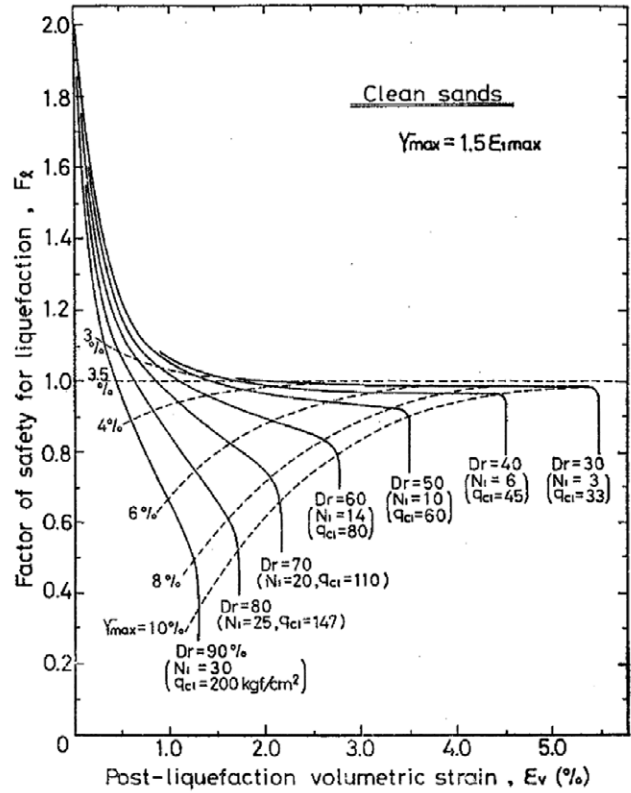


Figure 1. The combination of the safety factor, F_s , and post-liquefaction volumetric strain ε_v . (Modified from Ishihara and Yoshimine, 1992)

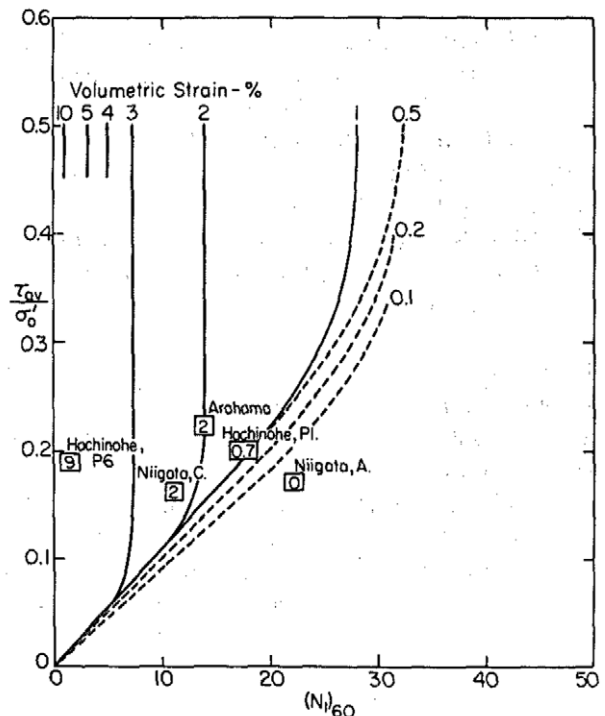


Figure 2. The relationship between corrected SPT, $(N_1)_{60}$, and volumetric strain (Modified from Tokimatsu and Seed, 1987)

According to the correlation, the intersection of D_R and PGA indicates the risk of liquefaction. In this context, “risk” means the frequency of liquefaction exposure. In Figure 3, the graph of the correlation is represented; and as can be seen, three zones of different risk levels are demonstrated on it. The first one is high-risk zone, which defines if the intersection of those is located at this zone, the study area has a high risk of liquefaction. The second zone is moderate-risk, which indicates that if the intersection point of the parameters is located in this zone, the study area has a moderate risk of liquefaction. Lastly, the third one is the non-liquefiable area. If the intersection of the parameters is in that zone, the study area is out of liquefaction risk.

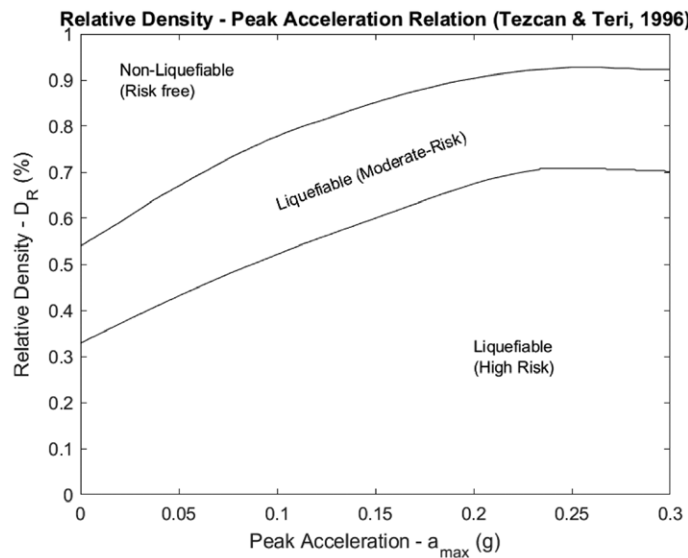


Figure 3. The graph of the relation between relative density (D_R) and peak ground acceleration (PGA). Modified from Tezcan and Teri (1996).

3. Overview of soilLique

soilLique is the first MATLAB® based program with GUI that ensures deterministic liquefaction analysis with the calculation of parameters that are previously propounded with the empirical equations.

The substantial feature of MATLAB® that makes it different from other programming tools is having a matrix-based language paving the way for computation of mathematical expressions. It provides an excellent environment for any courses (Chapra, 2012). Although other environments (e.g., Excel©) or languages (e.g., C++, Fortran 90) could have been chosen, MATLAB® presently offers a combination of convenient programming features with powerful built-in algorithms (Chapra, 2012). The user-friendly nature of MATLAB® explains why it is widely used to solve scientific and engineering problems. In addition to its user-friendly nature, having rich libraries (i.e., data and image processing tools) enlarges the implementation of MATLAB®. Graphical user interface (GUI) preference permits a code writer to create an interactive program that is semi-independent of MATLAB®. Specifically, one can construct a program in GUI, set it apart from MATLAB® and then, can run it after its installation to any computer provided that the installation of proper MATLAB® Runtime Environment version. The GUI feature is the glossy point of MATLAB®, which leads to soilLique. Moreover, MATLAB® allows users to switch between other languages. For example, a code written in MATLAB® can be converted to C++, Java, or other languages.

The algorithm presented here, soilLique, is designed for the mitigation of liquefaction triggered hazards based on four different calculation classes such as 1) SF analysis allowing estimation of SF of liquefaction with respect to shear wave velocity, SPT blow count data, and CPT data, 2) Settlement analysis that provides to evaluate calculations of settlements based on liquefaction, 3) The Evaluation of a Maximum Extent of a Liquefiable Area maintains predicting the distance of a liquefiable area to the epicenter or causative fault with corresponding earthquake magnitude, and lastly, 4) Simple analysis with only

considering relative density (D_R) and the peak ground acceleration (PGA) of the earthquake.

The workflow of the safety factor and settlement analyses part of soilLique is depicted in Figure 4. It can be inferred from the figure that soilLique has two main decision mechanisms. The first one is related to the specific part of the input file containing information on whether the soil structure includes fine or coarse particles. The second one is checking the shear wave velocity or SPT blow count values in both settlement and safety factor analyses.

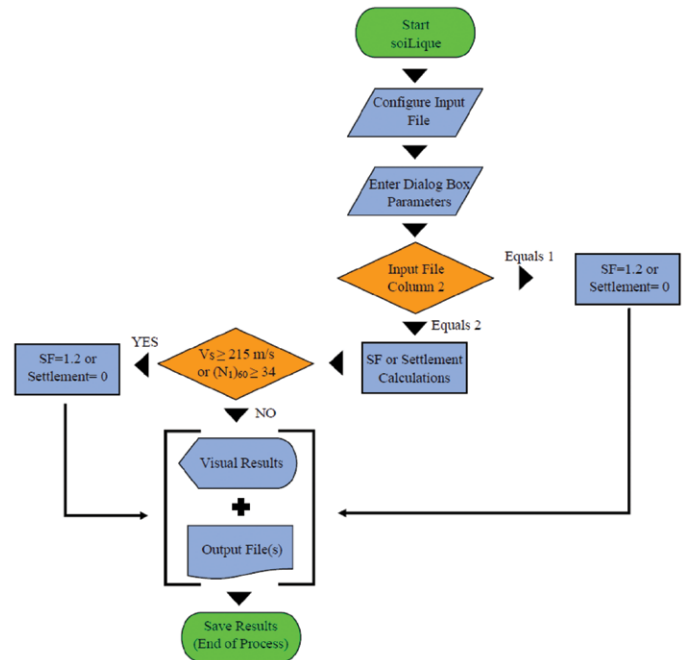


Figure 4. The workflow of soilLique for safety factor and settlement analyses.

These checking mechanisms are fundamentally based on the theoretical background of the program. In order to obey the calculation rules of formulas given in the theory section, soilLique has several limitations. These limitations are listed in Table 2.

In Table 2, “*terminate*” means considering safety factor as 1.2 and settlement as zero for the corresponding investigation depth. In the past, some liquefaction events have been observed while SF using related methods and assumptions were calculated to be greater than 1.00. In order to be on the safe side, it would be better to consider SF as 1.2. That is the reason why SF is capped to 1.2. Of course, this does not mean that liquefaction events will not be observed definitely for values higher than 1.2. Thus, it is a threshold value for the present study, and settlements are not expected for the values higher than 1.2. In the case of SF equals to 1.2, the program supposes that the subjected layer is non-liquefiable and terminates calculations of parameters for the corresponding layer. Then it continues to calculate liquefaction analysis parameters of the next layer/investigation depth. V_s based SF analysis is designed for calculations with or without FC data. The presumption of a limiting upper value of corrected shear wave velocity, V_{s1} , is considered as 215 m/s for areas with F.C. less than %5, and it is the same for the areas having F.C. values between %5 and %35. The upper limit for the shear wave velocity is considered as 200 m/s for areas having F.C. values equal to and greater than %35, according to the Equation 29. This limitation is a similar presumption that is commonly made in the SPT- and CPT-based procedures dealing with clean sands, where liquefaction is considered not possible (Andrus and Stokoe, 2000). If the F.C. data is accessible besides V_s measurements, one can consider it while creating the input file. In case of having no F.C. data, soilLique computes V_s based parameters based on Equation 27.

Additionally, there are several limitations to the calculation of the maximum distance of a liquefiable area, too. For instance, in the techniques of Wakamatsu (1991) and Wakamatsu (1993), the user must enter values higher than 5.0 for MJ as input. In addition to this issue, the user must recognize that soilLique only uses medium value calculations mentioned in Ulusay et al.

(2000), the upper boundary and lower boundary calculations are neglected in the present study.

Table 2. Limitations of soiLique

| Parameter / Method | Condition | Result / Calculation Status |
|--|------------------------------|-------------------------------|
| Safety Factor – SF | ≥ 1.2 | Non-Liquefiable / Terminates |
| | < 1.2 | Liquefiable / Continues |
| Corrected SPT Values – $(N_1)_{60}$ | ≥ 34 | Non- Liquefiable / Terminates |
| | < 34 | Liquefiable / Continues |
| Shear Wave Velocity – V_s | ≥ 215 m/s FC < %5 | Non- Liquefiable / Terminates |
| | ≥ 215 m/s %5 < FC < %35 | |
| | ≥ 200 m/s FC > %35 | |
| | < 215 m/s FC < %5 | Liquefiable / Continues |
| | < 215 m/s %5 < FC < %35 | |
| | < 200 m/s FC > %35 | |
| | ≥ 215 m/s without FC | |
| < 215 m/s without FC | Liquefiable / Continues | |
| Fine Content – FC | ≥ 35 | Non- Liquefiable / Terminates |
| | < 35 | Liquefiable / Continues |
| Water Table Level – h_w | $h_w > z$ | Liquefiable / Continues |
| | $h_w \leq z$ | Non- Liquefiable / Terminates |
| Wakamatsu (1991) | MJ < 5.0 | Terminates |
| | MJ > 5.0 | Continues |
| Wakamatsu (1993) | MJ < 5.0 | Terminates |
| | MJ > 5.0 | Continues |
| Ulusay et al. (2000) (*calculation of R) | MS < 5.5 | Terminates |
| | MS > 5.5 | Continues |

4. Results and Discussion

To test the robustness of soiLique, Soil Engineering, which was introduced by Ozcep (2010), was used for comparison. A real data set from Ozcep et al. (2014) is utilized in the present study for settlement and SPT-based analyses. Ozcep et al. (2014) have investigated to understand what role the soil properties play as one of the main factors causing earthquake damage in Yalova, and to compare the influence of two soil problems – amplification and liquefaction – on earthquake damage (Ozcep et al. 2014). All of the analysis sections, except settlement and SF analyses based on SPT data, were tested with synthetic data and presented under this heading.

4.1. Results of Real Data Set

The geological characteristics of Yalova can be explained by extensive Quaternary alluvial deposits, and the Tertiary Yalakdere and Kilic formations. Borehole locations are superimposed on the geological setting map in Figure 5. The Quaternary deposits consist of stratified materials having varied grain sizes and are derived from the various geological units in the vicinity (Yilmaz and Yavuzer 2005). The main drainage system is dominated by the Samanlı, Safran, Balaban, and Kazimiye rivers. Borehole records throughout the study

area show that the groundwater table is generally very shallow (Yilmaz and Yavuzer, 2005; Ozcep et al. 2014).

For the analysis process, the data obtained from three boreholes, BH43, BH76, and BH106, are used. Every analysis was carried out with the parameters M_w was considered as 7.4, and PGA was taken as 0.4 g. The water table levels of the boreholes, BH43, BH76, and BH106, are 2.65 m, 1.72 m, and 3.8 m, respectively. The map of the study area by indicating settlement distribution and locations of the selected boreholes is presented in Figure 6.

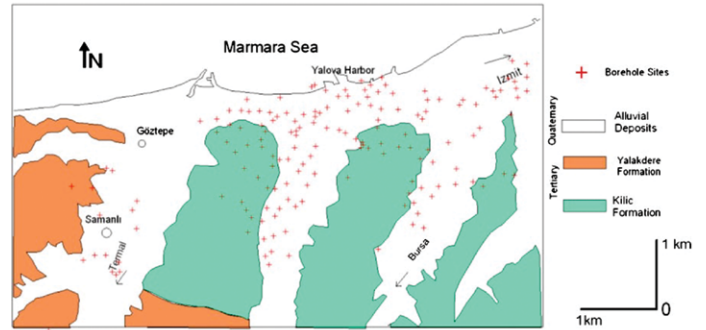


Figure 5. Map of the study region, including geological setting. Red plus signs correspond to borehole locations. Modified from Ozcep et al. (2014).

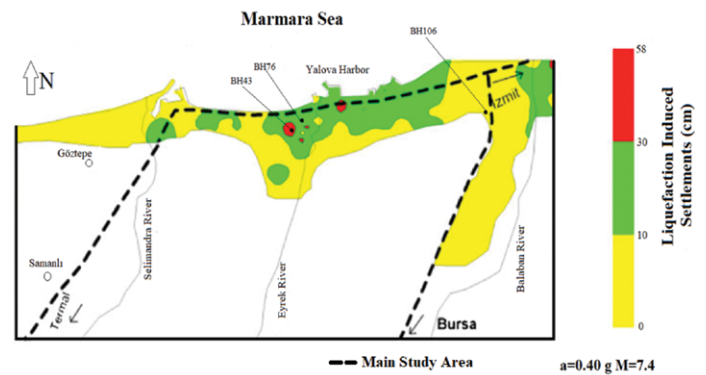


Figure 6. Map of liquefaction induced settlements of the study area using the Ishihara and Yoshimine (1992) approach. Black dots display locations of the boreholes, BH43, BH76, and BH106. Dashed lines show the boundary of the main study area. Modified from Ozcep et al. (2014).

According to the map presented in Figure 6, areas with the yellow color indicate the lowest amount of total settlement (0 - 10 cm) and, the green-colored areas correspond to middle settlement amounts (10 - 30 cm). Likewise, the red-colored areas have the highest amounts of settlement (30 - 58 cm). The selected three boreholes are relatively exemplary in terms of the amounts of different settlement quantities. The data of those boreholes were used to present a comparative study to test the robustness of soiLique.

One way to compare the results can be achieved by checking how close the layer-based settlement calculations of soiLique and SoilEngineering (Ozcep, 2010) for all boreholes. The settlement amount of each layer for the borehole, BH43, can be found in Table 3. Detailed tables for the calculations can be found in the supplementary data file. Additionally, the log plots for every borehole from soiLique, and SoilEngineering (Ozcep, 2010) are presented in Figure 7, Figure 8, and Figure 9 for boreholes BH43, BH76, BH106, respectively. These figures show that trends of the variation of SF with depth are consistent. As demonstrated in Table 3, the outputs of soiLique and SoilEngineering (Ozcep, 2010) are consistent with each other. For the total settlement comparisons, the results of both software show good agreement when taking all results and plots into consideration.

The layer-based settlement graphs are presented in Figure 10. These plots are specific to soiLique. Each row in Figure 10 corresponds to the results of boreholes, BH43, BH76, and BH106, respectively. These results were obtained by using the settlement analysis based on SPT. When SF varies below the safety

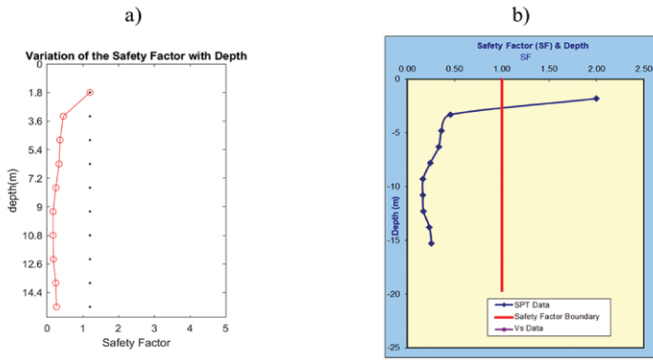


Figure 7. The variation of SF with depth for the borehole, BH43 a) from soilLique, b) from Soil Engineering (Ozcep, 2010).

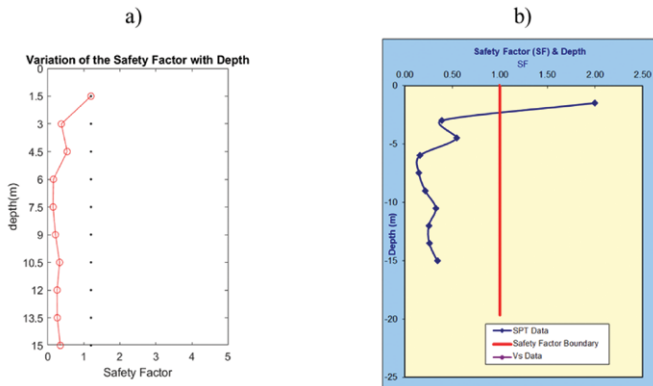


Figure 8. The variation of SF with depth for the borehole, BH76 a) from soilLique, b) from Soil Engineering (Ozcep, 2010).

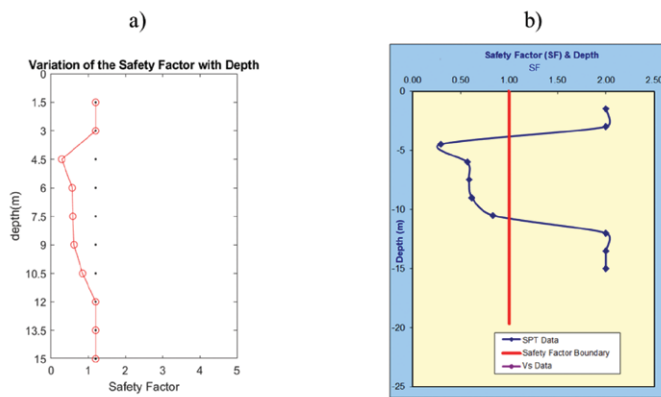


Figure 9. The variation of SF with depth for the borehole, BH106 a) from soilLique, b) from Soil Engineering (Ozcep, 2010).

limit, the layer-based settlements are calculated and plotted using two different approaches, such as ones introduced by Tokimatsu and Seed (1987) and Ishihara and Yoshimine (1992). On the far left of Figure 10, panels a, d, and g, the variation of settlement for each layer plots based on Tokimatsu and Seed (1987) approach is presented. The middle panels of Figure 10, b, e, and h, the variation of settlement for each layer plots depending on the Ishihara and Yoshimine (1992) approach is demonstrated. On the far right of Figure 10, panels c, f, and i represent the relationship between CRR and SPT ($N_{1,60}$) mentioned in Youd et al. (2001) is presented. soilLique represents that graph by putting a red circle where CRR and SPT ($N_{1,60}$) values intersect at a corresponding layer. As can be seen from the figures, these red circles were cumulated in or around the liquefiable region. It might be evidence of consistent calculation in terms of comparison of the already proven technique.

Another feature of soilLique is that plotting layer-based log plots showing liquefaction-prone layers. In Figure 11, liquefaction log plots of soilLique are demonstrated. In this figure, reds correspond to layers that are prone to liquefaction, and blues show safe layers. This kind of graphs helps the user to visualize the layers which may be prone to liquefaction. In Figure 4.7, panels from (a) to (c) are the representative of boreholes BH43, BH76, and BH106, respectively. Those logs are plotted with respect to SF values.

In addition to the layer-based settlement comparisons, the total settlements that were calculated by soilLique and SoilEngineering (Ozcep, 2010) were compared. A more detailed results table for the total settlement amounts is presented in the supplementary file. The total settlement amounts for every borehole calculated by soilLique, are presented in Table 4. Another way to test the robustness of the calculations done by soilLique can be achieved by using the map in Figure 6. For this testing process, the total amounts calculated by Ishihara and Yoshimine (1992) approach in Table 4 are focused only. As a result, the amounts calculated in the present study are consistent with the ranges represented in the color bar of the map. In detail, the borehole BH43 has the highest total settlement amount corresponding to the red-colored areas in Figure 6, and the borehole BH76 has the intermediate values as indicated by the green color on the map. The borehole BH106, which is located at the margin between Kilic Formation and alluvial deposits of Yalova, has the lowest total settlement amount as shown with yellow color on the map.

After pointing out the consistency between the results of soilLique and SoilEngineering (Ozcep, 2010), it would be better to mention the differences. It is obvious that small variations can be observed between the results presented in Table 3. These differences are related to the work procedures of soilLique and SoilEngineering (Ozcep, 2010). For example, soilLique assumes the highest limit for SF as 1.2, even though it is 2.0 in SoilEngineering (Ozcep, 2010). Besides, a slight difference can be observed between the results of the total vertical stress and the effective vertical stress in both software. Hence, these small differences affect CSR values. This fundamental difference occurs because soilLique considers the unit of the unit volume weight parameter as kN/m^2 , whereas SoilEngineering takes it as g/cm^3 . A comparative plot is presented in Figure 12 to show the trends of CSR and CRR values of both software. Although these differences have an impact on the calculations of the stress parameters -i.e., total vertical stress and effective vertical stress- and CSR values, it can be inferred from the figure that the mentioned differences can be neglectable. Lastly, the difference in the limitations for correction of the SPT values may cause some differences in CRR values. However, these effects are also negligible because the corresponding limits of the software are not far away from each other to affect the results negatively. These differences are valid for the V_s -based calculations, which can be observed from the V_s output tables in the supplementary file, and they can be neglected.

Table 3. Comparison of settlement results for BH43 calculated with soilLique and SoilEngineering (Ozcep, 2010)

| z (m) | soilLique Results | | SoilEngineering (Ozcep, 2010) Results | |
|------------|-------------------------------|---------------------------|---------------------------------------|---------------------------|
| | Ishihara and Yoshimine (1992) | Tokimatsu and Seed (1987) | Ishihara and Yoshimine (1992) | Tokimatsu and Seed (1987) |
| 1.8 | 0 | 0 | 0 | 0 |
| 3.3 | 4.88 | 3.99 | 4.89 | 4.01 |
| 4.8 | 5.15 | 4.37 | 5.14 | 4.35 |
| 6.3 | 5.14 | 4.35 | 5.14 | 4.35 |
| 7.8 | 6.31 | 6.2 | 6.3 | 6.18 |
| 9.3 | 7.95 | 11.7 | 7.95 | 11.7 |
| 10.8 | 8.06 | 12.35 | 8.05 | 12.3 |
| 12.3 | 7.96 | 11.76 | 7.95 | 11.7 |
| 13.8 | 6.64 | 6.73 | 6.64 | 6.72 |
| 15.3 | 6.52 | 6.53 | 6.53 | 6.54 |
| TOTAL (cm) | 58.62 | 67.98 | 58.59 | 67.85 |

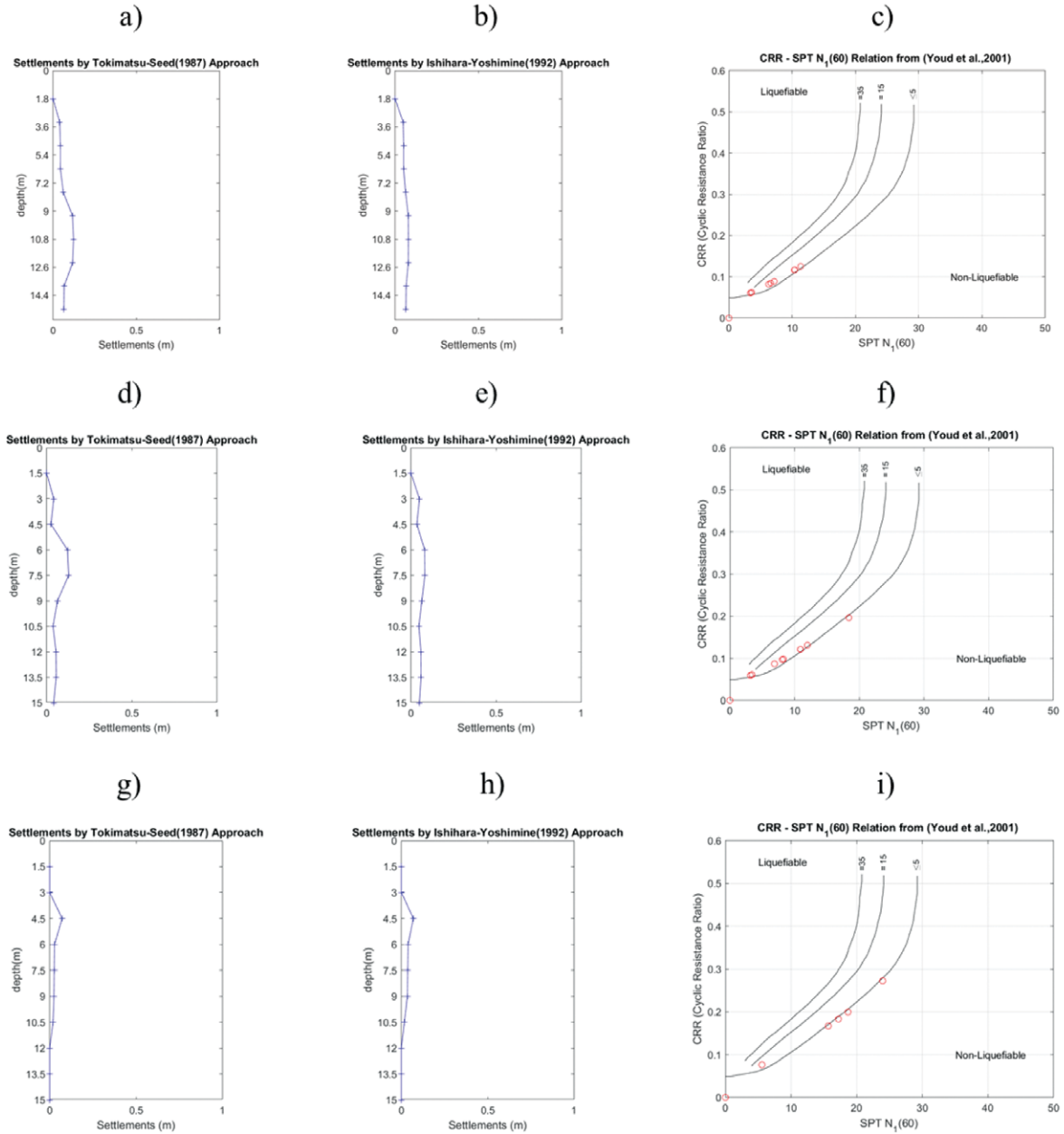


Figure 10. Other plots of results from soilLique. The first row (a, b, c) of the figure are the results for BH43 data, the second row (d, e, f) correspond to results of BH76 data, and the last row (g, h, i) shows the results of BH106 data. Panels a, d, g show the settlements for each layer with respect to Tokimatsu and Seed (1987) approach, and panels b, e, h show the settlements for each layer with respect to Ishihara and Yoshimine (1992) approach. Lastly, panels c, f, i show the CRR and $(N_1)_{60}$ relationship mentioned in Youd et al., (2001). This graph of relationship is digitized, and red circles correspond to CRR values.

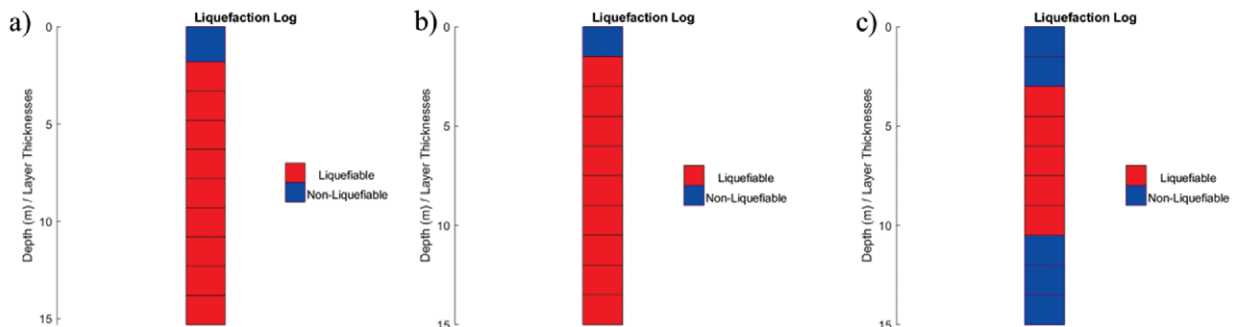


Figure 11. Liquefaction log plots from soilLique a) for BH43, b) for BH76 and c) for BH106

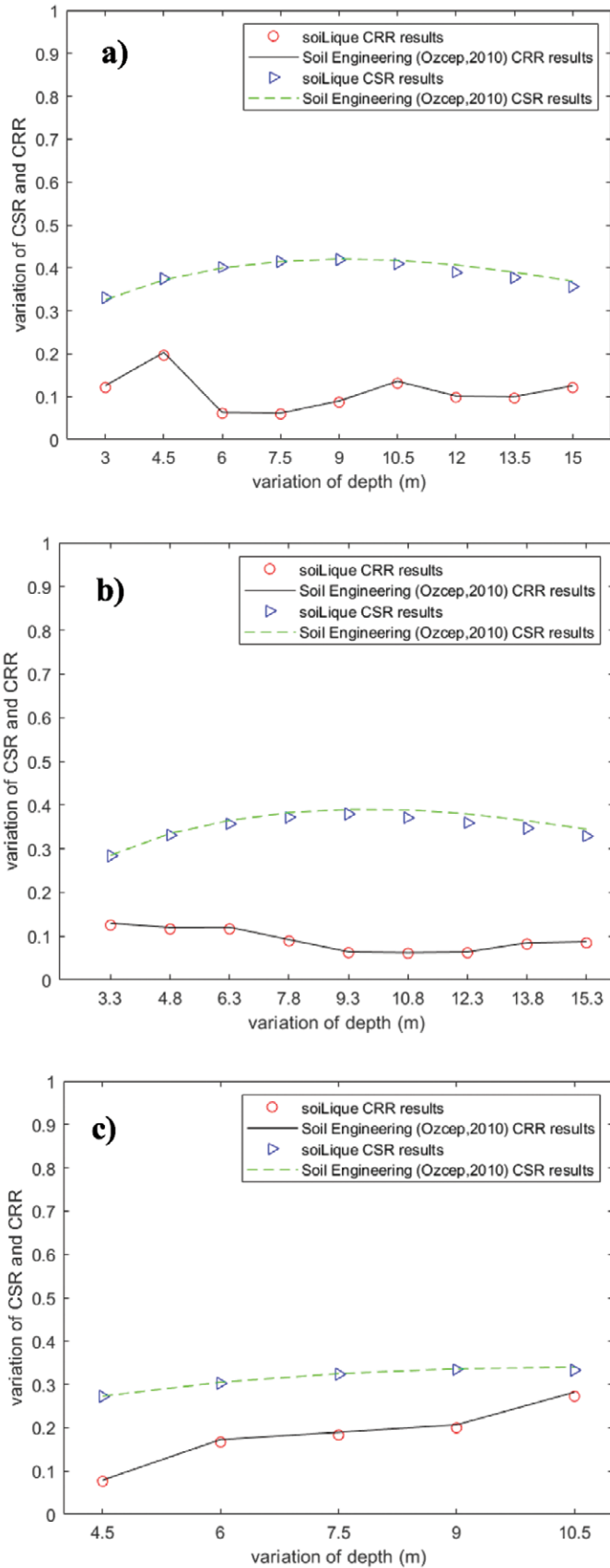


Figure 12. Comparative Plots of CRR and CSR results from soilLique and Soil Engineering for liquefiable layers of a) BH43, b) BH76, c) BH106. Red circles stand for soilLique CRR

Table 4. Table of total settlements calculated with soilLique for all boreholes.

| BH ID | Total Settlements | |
|-------|-------------------------------|---------------------------|
| | Ishihara and Yoshimine (1992) | Tokimatsu and Seed (1987) |
| BH43 | 58.62 cm | 67.98 cm |
| BH76 | 52.69 cm | 57.34 cm |
| BH106 | 19.72 cm | 17.06 cm |

Comparison of results from soilLique and SoilEngineering (Ozcep, 2010) reveals that although the work procedures of soilLique and SoilEngineering (Ozcep, 2010) may differ, the results are satisfactory.

4.2. Results of Synthetic Data Set

In the present study, the synthetic data set is used for showing results for safety factor analysis based on V_s values and CPT data. The safety factor analysis with respect to SPT data calculations of soilLique gives the same outputs except for settlement graphs and calculations.

Details of the input table and result table of safety factor analysis based on V_s analysis are presented in the supplementary file. The water table level is considered as 4.4 m, M_w is taken as 7.4, and PGA is accepted as 0.4 g for that calculation. In Figure 13, the results of the calculation based on V_s values are presented. That type of calculation has three visual outputs. One of them is the variation of SF with depth; the others are CRR- V_{s1} relation, which has been represented by Andrus and Stokoe (2000), and a liquefaction log plot. The limitation of the V_s based calculation is having the corrected shear wave velocities (V_s) below 215 m/s; in that case, the analysis will continue. However, if the corrected V_s values are higher than 215 m/s, the corresponding layer or layers will have SF equal to 1.2. In this example, all corrected V_s values are below this limit. That is the reason why all layers have SF below 1.2.

As well as the real SPT data set, the synthetic V_s data analysis is also checked with SoilEngineering (Ozcep, 2010). In this example, the fine content is not taken into consideration. Input and result tables of this analysis are demonstrated in the supplementary file. The plot of V_s -based analysis from SoilEngineering (Ozcep, 2010) is shown in Figure 14. In panel a, the screenshot of CSR results for V_s calculation from SoilEngineering is shown. As a comparison, both soilLique and SoilEngineering (Ozcep, 2010) consider the first two layers as not be prone to liquefaction. The trend of SF variations with depth is close to each other.

In addition to the synthetic V_s data analysis, an example analysis with synthetic CPT was carried out. In this synthetic example, the water table level is considered as 2.6 m, M_w is taken as 7.4, and PGA is accepted as 0.4 g for that calculation. Unfortunately, the results of the CPT data set could not be compared to any other programs because a free program that performs Suzuki et al. (1997) approach cannot be found. In Figure 15, the output of SF analysis based on synthetic CPT values are displayed. The routine presented here, soilLique, gives three types of visual outputs for CPT-based analysis. One of them is the variation of the SF with respect to depth; the others are CRR - q_{c1} relation that has been introduced by Suzuki et al. (1997) and the liquefaction log that shows which layers are liquefiable and which are not. CRR - q_{c1} relation graph is redrawn after digitizing the original plot, and soilLique adds points at intersections during the calculation.

In the second graph of Figure 15, one can observe that most of the red circles were gathered in the liquefiable region. These layers are responsive ones to liquefaction. That plot is one of the evidence for the calculation accuracy of soilLique.

A simple analysis can be carried out by using soilLique. In the presented algorithm, the output is a graph that is replotted from Tezcan and Teri (1996) with a red plus at the intersection point of those two parameters. For example, in this study, D_R is considered as 0.6 (%), and PGA is taken as 0.25 g to represent a plot. As a result, if the study area possesses D_R and PGA as or similar to those taken in that example, it means that the corresponding area has a substantial risk of liquefaction. The output of this example can be found in the supplementary file.

Lastly, the maximum extent of a liquefiable area was carried out as an example. The output can be found in the supplementary file. The theory

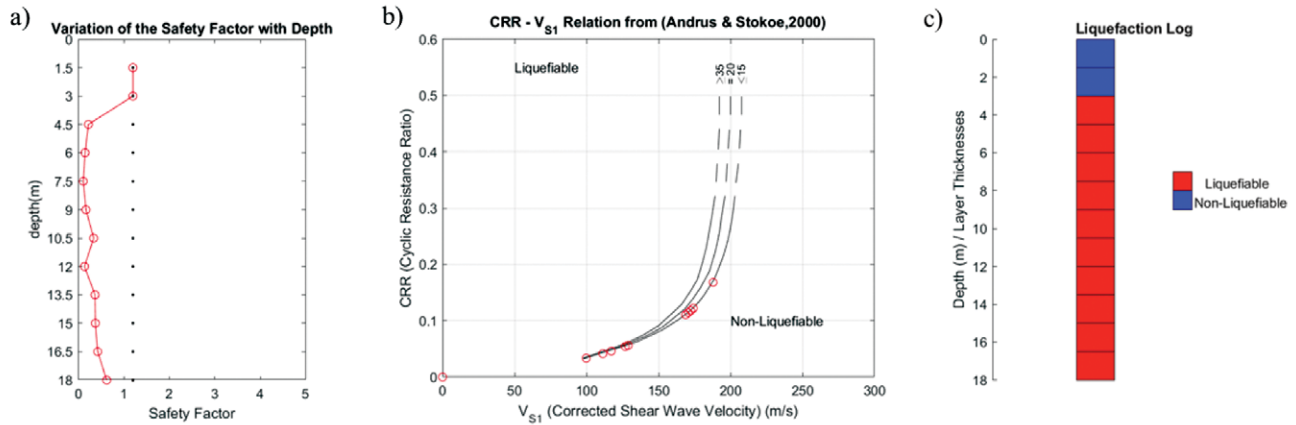


Figure 13. Outputs, from soilLique, for synthetic data that is used safety factor analysis based on V_s values. a) the variation of the safety factor with depth. b) the $CRR-V_{s1}$ relation that is taken from Andrus and Stokoe (2000) and redrawn with red circles at the intersection points. c) the liquefaction log. The water table level is considered as 4.4 m, $M_w=7.4$, and $PGA=0.4$ g.

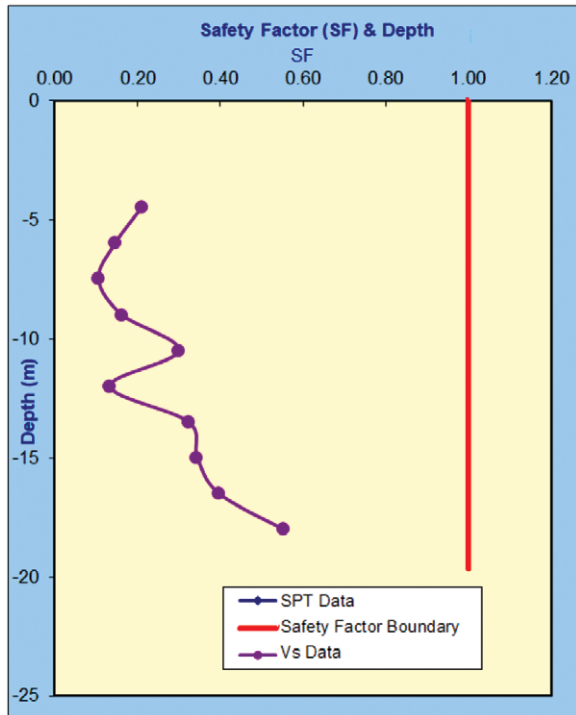


Figure 14. The graph of variation of SF with depth from SoilEngineering (Ozcep, 2010) for synthetic V_s data.

mentioned in Liu and Xie (1985) is used to calculate the maximum extent of a liquefiable area during an earthquake with M_L equals 6.7. As a result, the maximum extent is 23.945 km.

5. Conclusion

We have presented the first deterministic liquefaction analysis GUI written in MATLAB®. The capability of soilLique for performing liquefaction analysis is presented through two separate data sets, real and synthetic data. In order to check the robustness of soilLique, results were compared with another program, SoilEngineering (Ozcep, 2010). In terms of work procedure, soilLique and SoilEngineering (Ozcep, 2010) differs from each other.

Although SoilEngineering (Ozcep, 2010) has multiple calculation sections for a wide range of geotechnical problems, soilLique is focused only on deterministic liquefaction analyses. Moreover, soilLique includes alternative approaches for the calculation of the maximum extent of a liquefiable area, although SoilEngineering (Ozcep, 2010) includes only one of them. Likewise, soilLique provides to visualize the boreholes in terms of liquefaction.

The results demonstrate that soilLique obeys the limitations during calculations. For example, the choice of fine or coarse option in the second column of the input file directly affects the calculations as expected. In this study, the limitations of soilLique are presented in Table 3.1. As can be seen from the table, soil layers with SPT values greater than 34, and in most cases, the shear wave velocity greater than 215 m/s is accepted as non-liquifiable by soilLique. The limitation for F.C. is 35%, meaning that layers having F.C. lower than 35% is liquifiable. Additionally, it is evident that the limitations for Fine Content, SPT blow counts, V_s values, and the CPT-based calculations affect the results properly.

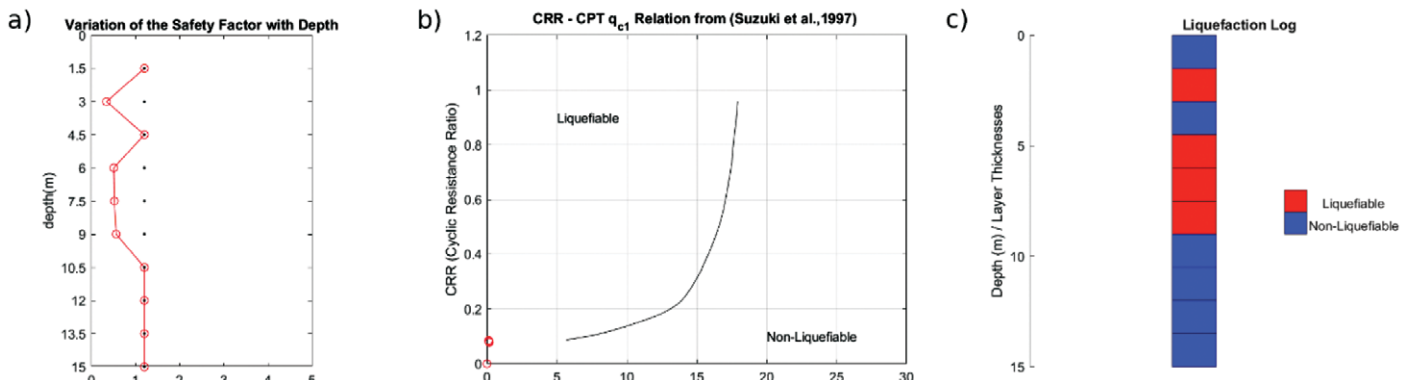


Figure 15. Outputs, from soilLique, for synthetic data that is used safety factor analysis based on CPT values. a) variation of the safety factor with depth. b) $CRR - q_{c1}$ relation is taken from Suzuki et al. (1997) and redrawn with red circles at the intersection points. c) liquefaction log. The water table level is considered as 2.6 m, $M_w=7.4$, and $PGA=0.4$ g.

Comparisons were made to check whether the results of soilLique and SoilEngineering (Ozcep, 2010) are consistent or not. These tests reveal that results were satisfactory and coincident with each other. That is to say; the calculated total settlement results yield a good agreement with the results of the previous study and SoilEngineering (Ozcep, 2010). The key features of soilLique are its easy-to-use nature, and being equipped with a variety of deterministic liquefaction analyses. In addition to these, its specific visual results make it easier to understand the liquefaction phenomenon for users. Consequently, soilLique is proven useful in terms of determination of the liquefaction triggered settlements and SF with short computation time.

6. Code Availability

soilLique is available as an open-source code and can be downloaded from the web site [<https://github.com/ekrembkn/soilLique>]. In the same directory, a user guide and examples can be found. It can be redistributed and/or modified under the terms of GNU Library General Public License 3.0. The user can download “soilLique.exe” to use it without MATLAB® instead of source codes, optionally.

Acknowledgments

This research was partly supported within the framework of the European LIQUEFACT project. The LIQUEFACT project has received funding from the European Union’s Horizon 2020 Research and Innovation Programme under Grant Agreement No. 700748.

References

- Ambraseys, N. N. (1988). Engineering seismology: part I. *Earthquake engineering & structural dynamics*, 17(1), 1-50. <https://doi.org/10.1002/eqe.4290170102>
- Andrus, R. D., & Stokoe II, K. H. (2000). Liquefaction resistance of soils from shear-wave velocity. *Journal of Geotechnical and Geoenvironmental engineering*, 126(11), 1015-1025. [https://doi.org/10.1061/\(ASCE\)1090-0241\(2000\)126:11\(1015\)](https://doi.org/10.1061/(ASCE)1090-0241(2000)126:11(1015))
- Bekin, E., & Ozcep, F. (2017). SoilLique: A MATLAB® Based Program to analyze soil Liquefaction and some applications/comparisons. *Proceedings of EGU General Assembly Conference Abstracts* (Vol. 19, p. 11868).
- Boulanger, R. W., & Idriss, I. M. (2014). CPT and SPT based liquefaction triggering procedures. *Report No. UCD/CGM.-14, 1*.
- Chapra, S. C. (2012). *Applied numerical methods with MATLAB for engineers and scientists*. New York: McGraw-Hill.
- Idriss, I. M., & Boulanger, R. W. (2008). *Soil liquefaction during earthquake*. Engineering monograph, EERI, California, USA, 266.
- Ishihara, K., & Yoshimine, M. (1992). Evaluation of settlements in sand deposits following liquefaction during earthquakes. *Soils and Foundations*, 32(1), 173-188. <https://doi.org/10.3208/sandf1972.32.173>
- Kuribayashi, E., & Tatsuoka, F. (1975). Brief review of liquefaction during earthquakes in Japan. *Soils and Foundations*, 15(4), 81-92. https://doi.org/10.3208/sandf1972.15.4_81
- Liao, S. S., & Whitman, R. V. (1986). Overburden correction factors for SPT in sand. *Journal of Geotechnical Engineering*, 112(3), 373-377. [https://doi.org/10.1061/\(ASCE\)0733-9410\(1986\)112:3\(373\)](https://doi.org/10.1061/(ASCE)0733-9410(1986)112:3(373))
- Liu, Y., & Xie, J. F. (1984). *Seismic liquefaction of sand*. Earthquake Pres, China.
- Mollamahmutoglu, M., & Babuccu, F. (2006). *Zeminlerde sivilasma analiz ve iyilestirme yontemleri*. Gazi Kitabevi.
- Ozcep, F. (2010). SoilEngineering: A Microsoft Excel® spreadsheet© program for geotechnical and geophysical analysis of soils. *Computers & Geosciences*, 36(10), 1355-1361. <https://doi.org/10.1016/j.cageo.2010.01.015>
- Ozcep, F., Karabulut, S., Ozel, O., Ozcep, T., Imre, N., & Zarif, H. (2014). Liquefaction-induced settlement, site effects and damage in the vicinity of Yalova City during the 1999 Izmit earthquake, Turkey. *Journal of Earth System Science*, 123(1), 73-89. <https://doi.org/10.1007/s12040-013-0387-7>
- Robertson, P. K., Woeller, D. J., & Finn, W. D. L. (1992). Seismic cone penetration test for evaluating liquefaction potential under cyclic loading. *Canadian Geotechnical Journal*, 29(4), 686-695. <https://doi.org/10.1139/t92-075>
- Seed, H. B., & Idriss, I. M. (1967). Analysis of soil liquefaction: Niigata earthquake. *Journal of the Soil Mechanics and Foundations Division*, 93(3), 83-108.
- Seed, H. B., & Idriss, I. M. (1971). Simplified procedure for evaluating soil liquefaction potential. *Journal of Soil Mechanics and Foundations*, 97(9), 249-1273. <https://doi.org/10.1061/JSFEAQ.0001662>
- Suzuki, Y., Koyamada, K., & Tokimatsu, K. (1997). *Prediction of liquefaction resistance based on CPT tip resistance and sleeve friction*. Proceedings, 14th International Conference on Soil Mechanics and Foundation Engineering, Hamburg, Germany, Vol. 1, pp. 603-606
- Sykora, D. W. (1987). *Creation of a data base of seismic shear wave velocity for correlation analysis*. Geotechnical Laboratory. Miscellaneous Paper GL-87-26, U.S. Army Engineer Waterways Experiment Station, Vicksburg, Miss.
- Terzaghi, K., & Peck, R. B. (1967). *Soil Mechanics in Engineering Practice*. Second ed. Wiley International Edition, New York 321pp.
- Tezcan, S., & Teri, L. (1996). *Shear wave propagation and liquefaction in layered soils, Türkiye Deprem Vakfı Yayınları, No: TDV*. TR 96-0005.
- Tokimatsu, K., & Seed, H. (1987). Evaluation of settlements in sands due to earthquake shaking. *Journal of Geotechnical Engineering*, 113(8), 861-878. [https://doi.org/10.1061/\(ASCE\)0733-9410\(1987\)113:8\(861\)](https://doi.org/10.1061/(ASCE)0733-9410(1987)113:8(861))
- Ulusay, R., Aydan, O., Kumsar, H., Sonmez, H., & Tuncay, E. (2000). Türkiye’de Son Depremlerde Gözlenen Sivilasma Olgusu ve Batı Anadolu’da Sivilasma Potansiyeline Genel Bir Bakış. Batı Anadolu’nun Depremselliği Sempozyumu. İzmir, Bildiriler Kitabı, 323-336.
- Yilmaz, I., & Yavuzer, D. (2005). Liquefaction potential and susceptibility mapping in the city of Yalova, Turkey. *Environmental Geology*, 47(2), 175-184. <https://doi.org/10.1007/s00254-004-1141-x>
- Youd, T. L., & Idriss, I. M. (1997). Proceedings of the NCEER workshop on evaluation of liquefaction resistance of soils.
- Youd, T. L., Idriss, I. M., Andrus, R. D., Arango, I., Castro, G., Christian, J. T., Dobry, R., Finn, W. D. L., Harder, L. F. Jr., Hynes, M. E., Ishihara, K., Koester, J. P., Liao, S. S. C., Marcuson, W. F. III., Martin, G. R., Mitchell, J. K., Moriwaki, Y., Power, M. S., Robertson, P. K., ... Stokoe, K. H. II. (2001). Liquefaction resistance of soils: summary report from the 1996 NCEER and 1998 NCEER/NSF workshops on evaluation of liquefaction resistance of soils. *Journal of Geotechnical Engineering*, 127(10), 817-833. [https://doi.org/10.1061/\(ASCE\)1090-0241\(2001\)127:10\(817\)](https://doi.org/10.1061/(ASCE)1090-0241(2001)127:10(817))

SUPPLEMENTARY DATA

A Comparative Soil Liquefaction Analysis with a MATLAB® based Algorithm: soilLique

In this supplementary data file, input tables and computation results for analyses carried out with real data and synthetic data were presented. In the first section, one can find the input and output tables of boreholes, BH34, BH76,

and BH106 were presented. These borehole data are used both in soilLique and SoilEngineering (Ozcep, 2010). The reader would find the liquefaction induced settlement (layer-based and total settlements) results for all boreholes in detail. In the second section, input tables and output tables for synthetic data are presented. After these tables, a screenshot figure of a simple analysis example and the maximum extent of a liquefiable area example were demonstrated.

1. REAL DATA

1.1. Settlement Analysis Based on SPT Data

Table S.1. Table of data input for BH43. The water table levels of BH43 is 2.65 m. M_w and PGA are considered as 7.4 and 0.4 g, respectively.

| z (m) | Fine (1) / Coarse(2) | SPT N | γ (kN/m ³) | C_u | C_b | C_r | C_s | Energy for C_e | Fine Content (%) |
|-------|----------------------|-------|-------------------------------|-------|-------|-------|-------|------------------|------------------|
| 1.8 | 1 | 8 | 18 | 1.7 | 1 | 1 | 0.8 | 45 | 82 |
| 3.3 | 2 | 7 | 18 | 1.37 | 1 | 1 | 0.8 | 45 | 30 |
| 4.8 | 2 | 6 | 18 | 1.24 | 1 | 1 | 0.8 | 45 | 39 |
| 6.3 | 2 | 8 | 18.5 | 1.14 | 1 | 1 | 0.8 | 45 | 25 |
| 7.8 | 2 | 7 | 18.9 | 1.06 | 1 | 1 | 0.8 | 45 | 15 |
| 9.3 | 2 | 6 | 19.2 | 1 | 1 | 1 | 0.8 | 45 | 5 |
| 10.8 | 2 | 6 | 19.5 | 0.94 | 1 | 1 | 0.8 | 45 | 3 |
| 12.3 | 2 | 6 | 19.8 | 0.9 | 1 | 1 | 0.8 | 45 | 8 |
| 13.8 | 2 | 7 | 20 | 0.86 | 1 | 1 | 0.8 | 45 | 15 |
| 15.3 | 2 | 8 | 20.5 | 0.82 | 1 | 1 | 0.8 | 45 | 15 |

Table S.2. Results of BH43 data calculated by soilLique. Settlements having (*) denotes Tokimatsu and Seed (1987) approach and (**) denotes Ishihara and Yoshimine (1992) approach.

| z (m) | σ | σ' | CSR | $(N_1)_{60}$ | $(N_1)_{60FC}$ | CRR | SF | Settlements* (m) | Settlements** (m) |
|-------|----------|-----------|--------|--------------|----------------|--------|------|------------------|-------------------|
| 1.8 | 32.4 | 32.4 | 0 | 0.0 | 0.0 | 0 | 1.20 | 0 | 0 |
| 3.3 | 59.4 | 53.0 | 0.2839 | 5.8 | 11.3 | 0.1252 | 0.46 | 0.0399 | 0.0488 |
| 4.8 | 86.4 | 65.3 | 0.3313 | 4.5 | 10.4 | 0.1163 | 0.36 | 0.0437 | 0.0515 |
| 6.3 | 116.55 | 80.7 | 0.3572 | 5.5 | 10.4 | 0.1166 | 0.34 | 0.0435 | 0.0514 |
| 7.8 | 147.42 | 96.9 | 0.372 | 4.5 | 7.2 | 0.089 | 0.25 | 0.062 | 0.0631 |
| 9.3 | 178.56 | 113.3 | 0.3792 | 3.6 | 3.6 | 0.0622 | 0.17 | 0.117 | 0.0795 |
| 10.8 | 210.6 | 130.6 | 0.3712 | 3.4 | 3.4 | 0.0608 | 0.17 | 0.1235 | 0.0806 |
| 12.3 | 243.54 | 148.9 | 0.3597 | 3.2 | 3.6 | 0.062 | 0.18 | 0.1176 | 0.0796 |
| 13.8 | 276 | 166.6 | 0.3469 | 3.6 | 6.3 | 0.0819 | 0.24 | 0.0673 | 0.0664 |
| 15.3 | 313.65 | 189.6 | 0.3293 | 3.9 | 6.6 | 0.0846 | 0.27 | 0.0653 | 0.0652 |

Table S.3. Input Data Table of BH76 for calculations in soilLique.

| z (m) | Fine (1) / Coarse(2) | SPT N | γ (kN/m ³) | C_u | C_b | C_r | C_s | Energy for C_e | Fine Content (%) |
|-------|----------------------|-------|-------------------------------|-------|-------|-------|-------|------------------|------------------|
| 1.5 | 2 | 4 | 17.5 | 1.7 | 1 | 1 | 0.8 | 45 | 80 |
| 3 | 2 | 6 | 18 | 1.37 | 1 | 1 | 0.8 | 45 | 80 |
| 4.5 | 2 | 15 | 18.3 | 1.24 | 1 | 1 | 0.8 | 45 | 75 |
| 6 | 2 | 5 | 18.3 | 1.14 | 1 | 1 | 0.8 | 45 | 2 |
| 7.5 | 2 | 5 | 18.5 | 1.06 | 1 | 1 | 0.8 | 45 | 5 |
| 9 | 2 | 7 | 18.8 | 1 | 1 | 1 | 0.8 | 45 | 15 |
| 10.5 | 2 | 12 | 19 | 0.94 | 1 | 1 | 0.8 | 45 | 26 |
| 12 | 2 | 8 | 19.5 | 0.9 | 1 | 1 | 0.8 | 45 | 20 |
| 13.5 | 2 | 5 | 19.5 | 0.86 | 1 | 1 | 0.8 | 45 | 70 |
| 15 | 2 | 10 | 19.9 | 0.82 | 1 | 1 | 0.8 | 45 | 94 |

Table S.4. SoiLique results table for BH76.

| z (m) | σ | σ' | CSR | $(N_1)_{60}$ | $(N_1)_{60FC}$ | CRR | SF | Settlements* (m) | Settlements** (m) |
|-------|----------|-----------|--------|--------------|----------------|--------|------|------------------|-------------------|
| 1.5 | 26.25 | 26.3 | 0 | 0.0 | 0.0 | 0 | 1.20 | 0 | 0 |
| 3 | 54 | 41.4 | 0.331 | 4.9 | 10.9 | 0.1213 | 0.38 | 0.0416 | 0.05 |
| 4.5 | 82.35 | 55.1 | 0.3754 | 11.2 | 18.4 | 0.1963 | 0.54 | 0.0253 | 0.0351 |
| 6 | 109.8 | 67.8 | 0.4017 | 3.4 | 3.4 | 0.061 | 0.16 | 0.1224 | 0.0804 |
| 7.5 | 138.75 | 82.0 | 0.4145 | 3.2 | 3.2 | 0.0595 | 0.15 | 0.1296 | 0.0816 |
| 9 | 169.2 | 97.8 | 0.4189 | 4.2 | 6.9 | 0.0869 | 0.21 | 0.0636 | 0.0641 |
| 10.5 | 199.5 | 113.4 | 0.4089 | 6.8 | 12.0 | 0.131 | 0.33 | 0.0376 | 0.0471 |
| 12 | 234 | 133.2 | 0.39 | 4.3 | 8.3 | 0.0983 | 0.26 | 0.0553 | 0.059 |
| 13.5 | 263.25 | 147.7 | 0.377 | 2.6 | 8.1 | 0.0967 | 0.27 | 0.0564 | 0.0596 |
| 15 | 298.5 | 168.2 | 0.3569 | 4.9 | 10.9 | 0.1212 | 0.35 | 0.0416 | 0.05 |

Table S.5. Input Data Table of BH106 for calculations in soiLique.

| z (m) | Fine (1) / Coarse(2) | SPT N | γ (kN/m ³) | C_n | C_b | C_r | C_s | Energy for C_c | Fine Content (%) |
|-------|----------------------|-------|-------------------------------|-------|-------|-------|-------|------------------|------------------|
| 1.5 | 2 | 6 | 18.5 | 1.7 | 1 | 1 | 0.8 | 45 | 8 |
| 3 | 2 | 7 | 18.5 | 1.37 | 1 | 1 | 0.8 | 45 | 6 |
| 4.5 | 2 | 7 | 19.7 | 1.24 | 1 | 1 | 0.8 | 45 | 8 |
| 6 | 2 | 13 | 20 | 1.14 | 1 | 1 | 0.8 | 45 | 99 |
| 7.5 | 2 | 16 | 20 | 1.06 | 1 | 1 | 0.8 | 45 | 100 |
| 9 | 2 | 19 | 20.5 | 1 | 1 | 1 | 0.8 | 45 | 100 |
| 10.5 | 2 | 28 | 20.7 | 0.94 | 1 | 1 | 0.8 | 45 | 100 |
| 12 | 2 | 42 | 21 | 0.9 | 1 | 1 | 0.8 | 45 | 98 |
| 13.5 | 2 | 45 | 21.5 | 0.86 | 1 | 1 | 0.8 | 45 | 99 |
| 15 | 2 | 46 | 22 | 0.82 | 1 | 1 | 0.8 | 45 | 100 |

Table S.6. SoiLique results table for BH106.

| z (m) | σ | σ' | CSR | $(N_1)_{60}$ | $(N_1)_{60FC}$ | CRR | SF | Settlements* (m) | Settlements** (m) |
|-------|----------|-----------|--------|--------------|----------------|--------|------|------------------|-------------------|
| 1.5 | 27.75 | 27.8 | 0 | 0.0 | 0.0 | 0 | 1.20 | 0 | 0 |
| 3 | 55.5 | 55.5 | 0 | 0.0 | 0.0 | 0 | 1.20 | 0 | 0 |
| 4.5 | 88.65 | 81.8 | 0.2721 | 5.2 | 5.6 | 0.0764 | 0.29 | 0.0716 | 0.0696 |
| 6 | 120 | 98.4 | 0.3025 | 8.9 | 15.7 | 0.1669 | 0.57 | 0.0282 | 0.0391 |
| 7.5 | 150 | 113.7 | 0.3233 | 10.2 | 17.2 | 0.1831 | 0.59 | 0.0265 | 0.0368 |
| 9 | 184.5 | 133.5 | 0.3346 | 11.4 | 18.7 | 0.1996 | 0.62 | 0.025 | 0.0346 |
| 10.5 | 217.35 | 151.6 | 0.3331 | 15.8 | 24.0 | 0.2725 | 0.85 | 0.0193 | 0.0171 |
| 12 | 252 | 171.6 | 0.326 | 22.7 | 32.2 | 0.7945 | 1.20 | 0 | 0 |
| 13.5 | 290.25 | 195.1 | 0.3147 | 23.2 | 32.9 | 1.1191 | 1.20 | 0 | 0 |
| 15 | 330 | 220.1 | 0.3015 | 22.6 | 32.2 | 0.7766 | 1.20 | 0 | 0 |

Table S.7. SoilEngineering (Ozcep, 2010) SPT-based liquefaction analysis panel. Red numbers are inputs for CSR calculations of BH43.

The water table level of BH43 is 2.65 m. $M_w=7.4$, $PGA=0.4$ g.

| Depth (m) | γ (g/cm ³) | Fine Content (%) | σ (kPa) | σ' (kPa) | r_d | CSR |
|-----------|-------------------------------|------------------|----------------|-----------------|-----------|-------|
| 1.8 | 1.8 | 82 | 31.8 | 31.8 | 0.988147 | 0.257 |
| 3.3 | 1.8 | 30 | 58.3 | 51.9 | 0.9773893 | 0.285 |
| 4.8 | 1.8 | 39 | 84.8 | 63.7 | 0.9669309 | 0.335 |
| 6.3 | 1.85 | 25 | 112 | 76.2 | 0.9551352 | 0.365 |
| 7.8 | 1.89 | 15 | 139.8 | 89.3 | 0.9397014 | 0.383 |
| 9.3 | 1.92 | 5 | 168 | 102.8 | 0.9179441 | 0.39 |
| 10.8 | 1.95 | 3 | 196.7 | 116.8 | 0.8875651 | 0.389 |
| 12.3 | 1.98 | 8 | 225.9 | 131.2 | 0.8478937 | 0.38 |
| 13.8 | 2 | 15 | 255.3 | 145.9 | 0.8008678 | 0.364 |
| 15.3 | 2.05 | 15 | 285.5 | 161.4 | 0.7507104 | 0.345 |

Table S.8. SoilEngineering (Ozcep, 2010) SPT-based liquefaction analysis panel. Red numbers are inputs for CRR calculations of BH43. The water table level of BH43 is 2.65 m. $M_w=7.4$, $PGA=0.4$ g.

| Depth (m) | SPT (field) | C_n | C_e | C_b | C_r | C_s | $(N_1)_{L60FC}$ | CRR | SF |
|-----------|-------------|-------|-------|-------|-------|-------|-----------------|--------|------|
| 1.8 | 8 | 1.7 | 0.75 | 1 | 1 | 0.8 | 13.3 | 0.1486 | 2 |
| 3.3 | 7 | 1.37 | 0.75 | 1 | 1 | 0.8 | 11.3 | 0.1296 | 0.45 |
| 4.8 | 6 | 1.24 | 0.75 | 1 | 1 | 0.8 | 10.4 | 0.1203 | 0.36 |
| 6.3 | 8 | 1.14 | 0.75 | 1 | 1 | 0.8 | 10.4 | 0.1206 | 0.33 |
| 7.8 | 7 | 1.06 | 0.75 | 1 | 1 | 0.8 | 7.2 | 0.0921 | 0.24 |
| 9.3 | 6 | 1 | 0.75 | 1 | 1 | 0.8 | 3.6 | 0.0644 | 0.16 |
| 10.8 | 6 | 0.94 | 0.75 | 1 | 1 | 0.8 | 3.4 | 0.0629 | 0.16 |
| 12.3 | 6 | 0.9 | 0.75 | 1 | 1 | 0.8 | 3.6 | 0.0642 | 0.17 |
| 13.8 | 7 | 0.86 | 0.75 | 1 | 1 | 0.8 | 6.3 | 0.0848 | 0.23 |
| 15.3 | 8 | 0.82 | 0.75 | 1 | 1 | 0.8 | 6.6 | 0.0876 | 0.25 |

Table S.9. SoilEngineering (Ozcep, 2010) SPT-based liquefaction analysis panel. Red numbers are inputs for CSR calculations of BH76. The water table level of BH76 is 1.72 m. $M_w=7.4$, $PGA=0.4$ g.

| Depth (m) | γ (g/cm ³) | Fine Content (%) | σ (kPa) | σ' (kPa) | r_d | CSR |
|-----------|-------------------------------|------------------|----------------|-----------------|-----------|-------|
| 1.5 | 1.75 | 80 | 30.9 | 30.9 | 0.9904198 | 0.258 |
| 3 | 1.8 | 80 | 57.4 | 44.8 | 0.9794776 | 0.326 |
| 4.5 | 1.83 | 75 | 84.3 | 57 | 0.9690669 | 0.372 |
| 6 | 1.83 | 2 | 111.2 | 69.3 | 0.9577033 | 0.4 |
| 7.5 | 1.85 | 5 | 138.5 | 81.8 | 0.943207 | 0.415 |
| 9 | 1.88 | 15 | 166.1 | 94.7 | 0.9229267 | 0.421 |
| 10.5 | 1.9 | 26 | 194.1 | 108 | 0.8943968 | 0.418 |
| 12 | 1.95 | 20 | 222.8 | 121.9 | 0.8565184 | 0.407 |
| 13.5 | 1.95 | 70 | 251.5 | 135.9 | 0.8106803 | 0.39 |
| 15 | 1.99 | 94 | 280.8 | 150.5 | 0.7607536 | 0.369 |

Table S.10. SoilEngineering (Ozcep, 2010) SPT-based liquefaction analysis panel. Red numbers are inputs for CRR calculations of BH76. The water table level of BH76 is 1.72 m. $M_w=7.4$, $PGA=0.4$ g.

| Depth (m) | SPT (field) | C_n | C_e | C_b | C_r | C_s | $(N_1)_{L60FC}$ | CRR | SF |
|-----------|-------------|-------|-------|-------|-------|-------|-----------------|--------|------|
| 1.5 | 4 | 1.7 | 0.75 | 1 | 1 | 0.8 | 9.2 | 0.1095 | 2 |
| 3 | 6 | 1.37 | 0.75 | 1 | 1 | 0.8 | 10.9 | 0.1255 | 0.39 |
| 4.5 | 15 | 1.24 | 0.75 | 1 | 1 | 0.8 | 18.4 | 0.2031 | 0.55 |
| 6 | 5 | 1.14 | 0.75 | 1 | 1 | 0.8 | 3.4 | 0.0631 | 0.16 |
| 7.5 | 5 | 1.06 | 0.75 | 1 | 1 | 0.8 | 3.2 | 0.0616 | 0.15 |
| 9 | 7 | 1 | 0.75 | 1 | 1 | 0.8 | 6.9 | 0.0899 | 0.21 |
| 10.5 | 12 | 0.94 | 0.75 | 1 | 1 | 0.8 | 12 | 0.1356 | 0.32 |
| 12 | 8 | 0.9 | 0.75 | 1 | 1 | 0.8 | 8.3 | 0.1017 | 0.25 |
| 13.5 | 5 | 0.86 | 0.75 | 1 | 1 | 0.8 | 8.1 | 0.1001 | 0.26 |
| 15 | 10 | 0.82 | 0.75 | 1 | 1 | 0.8 | 10.9 | 0.1254 | 0.34 |

Table S.11. SoilEngineering (Ozcep, 2010) SPT-based liquefaction analysis panel. Red numbers are inputs for CSR calculations of BH76. The water table level of BH106 is 3.8 m. $M_w=7.4$, $PGA=0.4$ g.

| Depth (m) | γ (g/cm ³) | Fine Content (%) | σ (kPa) | σ' (kPa) | r_d | CSR |
|-----------|-------------------------------|------------------|----------------|-----------------|-----------|-------|
| 1.5 | 1.85 | 8 | 32.7 | 32.7 | 0.9904198 | 0.258 |
| 3 | 1.85 | 6 | 59.9 | 59.9 | 0.9794776 | 0.255 |
| 4.5 | 1.97 | 8 | 88.9 | 82 | 0.9690669 | 0.273 |
| 6 | 2 | 99 | 118.3 | 96.7 | 0.9577033 | 0.305 |
| 7.5 | 2 | 100 | 147.7 | 111.4 | 0.943207 | 0.325 |
| 9 | 2.05 | 100 | 177.9 | 126.9 | 0.9229267 | 0.336 |
| 10.5 | 2.07 | 100 | 208.4 | 142.6 | 0.8943968 | 0.34 |
| 12 | 2.1 | 98 | 239.3 | 158.8 | 0.8565184 | 0.335 |
| 13.5 | 2.15 | 99 | 270.9 | 175.7 | 0.8106803 | 0.325 |
| 15 | 2.2 | 100 | 303.3 | 193.4 | 0.7607536 | 0.31 |

Table S.12. Soil Engineering (Ozcep, 2010) SPT-based liquefaction analysis panel. Red numbers are inputs for CRR calculations of BH76. The water table level of BH106 is 3.8 m. $M_w=7.4$, $PGA=0.4$ g.

| Depth (m) | SPT (field) | C_n | C_e | C_b | C_r | C_s | (N_{L60FC}) | CRR | SF |
|-----------|-------------|-------|-------|-------|-------|-------|---------------|--------|------|
| 1.5 | 6 | 1.7 | 0.75 | 1 | 1 | 0.8 | 5.6 | 0.079 | 2 |
| 3 | 7 | 1.37 | 0.75 | 1 | 1 | 0.8 | 5.8 | 0.081 | 2 |
| 4.5 | 7 | 1.24 | 0.75 | 1 | 1 | 0.8 | 5.6 | 0.0791 | 0.29 |
| 6 | 13 | 1.14 | 0.75 | 1 | 1 | 0.8 | 15.7 | 0.1727 | 0.57 |
| 7.5 | 16 | 1.06 | 0.75 | 1 | 1 | 0.8 | 17.2 | 0.1895 | 0.58 |
| 9 | 19 | 1 | 0.75 | 1 | 1 | 0.8 | 18.7 | 0.2066 | 0.6 |
| 10.5 | 28 | 0.94 | 0.75 | 1 | 1 | 0.8 | 24 | 0.2821 | 0.83 |
| 12 | 42 | 0.9 | 0.75 | 1 | 1 | 0.8 | 32.2 | 0.55 | SY |
| 13.5 | 45 | 0.86 | 0.75 | 1 | 1 | 0.8 | 32.9 | 0.55 | SY |
| 15 | 46 | 0.82 | 0.75 | 1 | 1 | 0.8 | 32.2 | 0.55 | SY |

Table S.13. Liquefaction Induced Settlements table for each layers of all boreholes

| z (m) | soiLique Results | | Soil Engineering (Ozcep, 2010) Results | | |
|--------------|-------------------------------|---------------------------|--|---------------------------|-----------------------|
| | Ishihara and Yoshimine (1992) | Tokimatsu and Seed (1987) | Ishihara and Yoshimine (1992) | Tokimatsu and Seed (1987) | |
| 1.8 | 0 | 0 | 0 | 0 | Settlements for BH43 |
| 3.3 | 4.88 | 3.99 | 4.89 | 4.01 | |
| 4.8 | 5.15 | 4.37 | 5.14 | 4.35 | |
| 6.3 | 5.14 | 4.35 | 5.14 | 4.35 | |
| 7.8 | 6.31 | 6.2 | 6.3 | 6.18 | |
| 9.3 | 7.95 | 11.7 | 7.95 | 11.7 | |
| 10.8 | 8.06 | 12.35 | 8.05 | 12.3 | |
| 12.3 | 7.96 | 11.76 | 7.95 | 11.7 | |
| 13.8 | 6.64 | 6.73 | 6.64 | 6.72 | |
| 15.3 | 6.52 | 6.53 | 6.53 | 6.54 | |
| TOTAL | 58.62 | 67.98 | 58.59 | 67.85 | |
| 1.5 | 0 | 0 | 0 | 0 | Settlements for BH76 |
| 3 | 5 | 4.16 | 5 | 4.16 | |
| 4.5 | 3.51 | 2.53 | 3.51 | 2.52 | |
| 6 | 8.04 | 12.24 | 8.05 | 12.3 | |
| 7.5 | 8.16 | 12.96 | 8.15 | 12.9 | |
| 9 | 6.41 | 6.36 | 6.41 | 6.36 | |
| 10.5 | 4.71 | 3.76 | 4.7 | 3.75 | |
| 12 | 5.9 | 5.53 | 5.89 | 5.52 | |
| 13.5 | 5.96 | 5.64 | 5.96 | 5.64 | |
| 15 | 5 | 4.16 | 5 | 4.16 | |
| TOTAL | 52.69 | 57.34 | 52.67 | 57.31 | |
| 1.5 | 0 | 0 | 0 | 0 | Settlements for BH106 |
| 3 | 0 | 0 | 0 | 0 | |
| 4.5 | 6.96 | 7.16 | 6.95 | 7.14 | |
| 6 | 3.91 | 2.82 | 3.9 | 2.81 | |
| 7.5 | 3.68 | 2.65 | 3.68 | 2.65 | |
| 9 | 3.46 | 2.5 | 3.46 | 2.49 | |
| 10.5 | 1.71 | 1.93 | 1.77 | 1.93 | |
| 12 | 0 | 0 | 0 | 0 | |
| 13.5 | 0 | 0 | 0 | 0 | |
| 15 | 0 | 0 | 0 | 0 | |
| TOTAL | 19.72 | 17.06 | 19.76 | 17.02 | |

2. SYNTHETIC DATA

2.1. Synthetic V_s Data

Table S.14. Input table for synthetic data that is used safety factor analysis based on synthetic V_s values. The water table level is considered as 4.4 m, $M_w=7.4$, and $PGA=0.4$ g.

| z(m) | Fine (1) / Coarse (2) | γ (kN/m ³) | V_s (m/s) |
|-------|-----------------------|-------------------------------|-------------|
| 1.50 | 1.00 | 19.00 | 200.00 |
| 3.00 | 2.00 | 19.00 | 210.00 |
| 4.50 | 2.00 | 18.00 | 120.00 |
| 6.00 | 2.00 | 18.50 | 110.00 |
| 7.50 | 2.00 | 17.50 | 100.00 |
| 9.00 | 2.00 | 16.50 | 130.00 |
| 10.50 | 2.00 | 18.00 | 180.00 |
| 12.00 | 2.00 | 17.00 | 125.00 |
| 13.50 | 2.00 | 18.00 | 192.00 |
| 15.00 | 2.00 | 19.00 | 198.00 |
| 16.50 | 2.00 | 20.00 | 210.00 |
| 18.00 | 2.00 | 21.00 | 235.00 |

Table S.15. Table of results for safety factor analysis based on synthetic V_s values.

| σ | σ' | CSR | V_{s1} (m/s) | CRR | SF |
|----------|-----------|--------|----------------|--------|--------|
| 28.5 | 28.5 | 0 | 0 | 0 | 1.2 |
| 57 | 57 | 0 | 0 | 0 | 1.2 |
| 81 | 80.019 | 0.2541 | 126.877 | 0.0542 | 0.2205 |
| 111 | 95.304 | 0.2889 | 111.3307 | 0.0413 | 0.1477 |
| 131.25 | 100.839 | 0.319 | 99.7913 | 0.0332 | 0.1076 |
| 148.5 | 103.374 | 0.3478 | 128.926 | 0.0561 | 0.1668 |
| 189 | 129.159 | 0.34 | 168.8462 | 0.1104 | 0.3358 |
| 204 | 129.444 | 0.3498 | 117.1897 | 0.0458 | 0.1355 |
| 243 | 153.729 | 0.3344 | 172.4298 | 0.1182 | 0.3656 |
| 285 | 181.014 | 0.3166 | 170.7014 | 0.1143 | 0.3734 |
| 330 | 211.299 | 0.2978 | 174.1787 | 0.1223 | 0.4249 |
| 378 | 244.584 | 0.2786 | 187.9147 | 0.168 | 0.624 |

Table S.16. SoilEngineering (Ozcep, 2010) V_s -based liquefaction analysis panel. Red numbers are inputs for CSR calculations. The water table level is considered as 4.4 m, $M_w=7.4$, and $PGA=0.4$ g.

| Depth (m) | γ (g/cm ³) | σ (kPa) | σ' (kPa) | r_d | CSR |
|-----------|-------------------------------|----------------|-----------------|-----------|-------|
| 1.5 | 1.9 | 33.6 | 33.6 | 0.9904198 | 0.258 |
| 3 | 1.9 | 61.5 | 61.5 | 0.9794776 | 0.255 |
| 4.5 | 1.8 | 88 | 87 | 0.9690669 | 0.255 |
| 6 | 1.85 | 115.2 | 99.5 | 0.9577033 | 0.288 |
| 7.5 | 1.75 | 141 | 110.6 | 0.943207 | 0.313 |
| 9 | 1.65 | 165.2 | 120.1 | 0.9229267 | 0.33 |
| 10.5 | 1.8 | 191.7 | 131.9 | 0.8943968 | 0.338 |
| 12 | 1.7 | 216.8 | 142.2 | 0.8565184 | 0.339 |
| 13.5 | 1.8 | 243.2 | 154 | 0.8106803 | 0.333 |
| 15 | 1.9 | 271.2 | 167.2 | 0.7607536 | 0.321 |
| 16.5 | 2 | 300.6 | 181.9 | 0.711582 | 0.306 |
| 18 | 2.1 | 331.5 | 198.1 | 0.6670533 | 0.29 |

Table S.17. SoilEngineering (Ozcep, 2010) V_s -based liquefaction analysis panel. Red numbers are inputs for CRR calculations. The water table level is considered as 4.4 m, $M_w=7.4$, and $PGA=0.4$ g.

| Depth (m) | V_s (m/s) | C_v | V_{s1} (m/s) | V_{s1c} (m/s) | CRR | SF |
|-----------|-------------|-------|----------------|-----------------|--------|--------|
| 1.5 | 200 | 1.31 | SY | 220 | SY* | SY* |
| 3 | 210 | 1.13 | SY | 220 | SY* | SY* |
| 4.5 | 120 | 1.04 | 124.25 | 220 | 0.0534 | 0.2097 |
| 6 | 110 | 1 | 110.13 | 220 | 0.0419 | 0.1454 |
| 7.5 | 100 | 0.98 | 97.52 | 220 | 0.0329 | 0.1052 |
| 9 | 130 | 0.96 | 124.18 | 220 | 0.0534 | 0.1617 |
| 10.5 | 180 | 0.93 | 167.96 | 220 | 0.1013 | 0.2995 |
| 12 | 125 | 0.92 | 114.47 | 220 | 0.0453 | 0.1334 |
| 13.5 | 192 | 0.9 | 172.36 | 220 | 0.1076 | 0.323 |
| 15 | 198 | 0.88 | 174.12 | 220 | 0.1102 | 0.3435 |
| 16.5 | 210 | 0.86 | 180.82 | 220 | 0.1211 | 0.396 |
| 18 | 235 | 0.84 | 198.08 | 220 | 0.1601 | 0.5516 |

*SY means properties of the layer exceeds the upper limit for liquefaction calculation.

2.2. Synthetic CPT Data

Table S.18. Input data table for the safety factor analysis based on synthetic CPT data. The water table level is considered as 2.6 m, $M_w=7.4$ and $PGA=0.4$ g.

| z(m) | Fine (1) / Coarse(2) | γ | q_c (mPa) | f_s (mPa) |
|-------|----------------------|----------|-------------|-------------|
| 1.50 | 1.00 | 19.00 | 5.00 | 0.05 |
| 3.00 | 2.00 | 17.00 | 8.00 | 0.03 |
| 4.50 | 1.00 | 18.00 | 10.00 | 0.08 |
| 6.00 | 2.00 | 16.00 | 12.00 | 0.10 |
| 7.50 | 2.00 | 17.00 | 13.00 | 0.09 |
| 9.00 | 2.00 | 16.80 | 15.00 | 0.15 |
| 10.50 | 1.00 | 18.00 | 13.00 | 0.12 |
| 12.00 | 1.00 | 17.80 | 17.00 | 0.16 |
| 13.50 | 1.00 | 18.00 | 16.00 | 0.14 |
| 15.00 | 1.00 | 19.00 | 18.00 | 0.16 |

Table S.19. Table of results for safety factor analysis based on synthetic CPT values.

| σ | σ' | CSR | CRR | SF | q_{c1} (mPa) |
|----------|-----------|----------|----------|--------|----------------|
| 28.5 | 0 | 0 | 0 | 1.2 | 0 |
| 51 | 47 | 0.028128 | 0.084974 | 0.3425 | 0.1167 |
| 81 | 0 | 0 | 0 | 1.2 | 0 |
| 96 | 62 | 0.039194 | 0.079895 | 0.5075 | 0.1524 |
| 127.5 | 78.5 | 0.040619 | 0.080669 | 0.5209 | 0.1467 |
| 151.2 | 87.2 | 0.042835 | 0.078793 | 0.5624 | 0.1606 |
| 189 | 0 | 0 | 0 | 1.2 | 0 |
| 213.6 | 0 | 0 | 0 | 1.2 | 0 |
| 243 | 0 | 0 | 0 | 1.2 | 0 |
| 285 | 0 | 0 | 0 | 1.2 | 0 |

2.3. Synthetic Example Result of Simple Analysis (Tezcan & Teri, 1996)

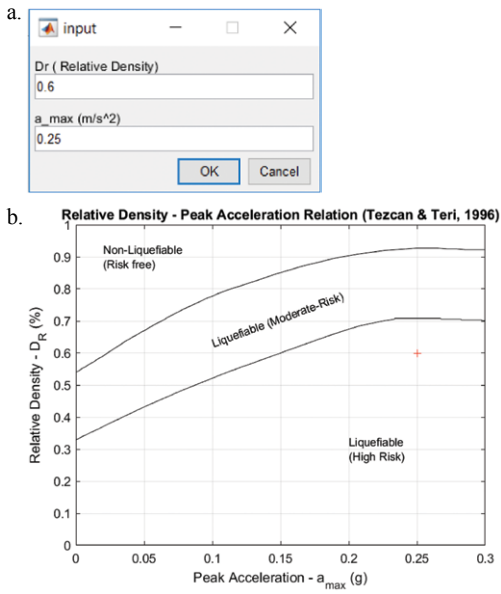


Figure S1. a) input b) the result of simple analysis. Graph is digitized and replotted from Tezcan and Teri (1996). The red plus is an indication of the intersection point.

2.4. Synthetic Example for the Maximum Extent of a Liquefiable Area Analysis

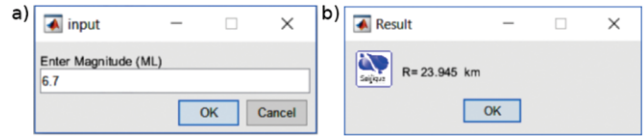


Figure S2. a) input and b) output dialogue box for the maximum extent analysis with the theory of Liu and Xie (1985).